MONASH University
Institute of Pharmaceutical Sciences

HaloTag pseudotyped lentivirus: Quantifying uptake and internalisation in vitro using a fluorescent click sensor

Jia Yi Kuah

B. Pharmaceutical Sciences Advanced (Hons) Monash University

A thesis submitted for the degree of

Master of Philosophy

at

Monash University in 2022

Drug Delivery, Disposition and Dynamics,

Monash Institute of Pharmaceutical Science

Copyright notice

Table of Contents

Copyright notice ..... ***i***

Table of Contents ..... ***ii***

Abstract ..... ***v***

Declaration ..... ***vii***

Acknowledgements ..... ***viii***

Abbreviations ..... ***ix***

1. Chapter 1. Introduction ***1***

1.1 General Introduction **1**

1.1.1 Statement of the problem 1

1.1.2 Nanoparticle Internalisation Pathways 2

1.1.3 Viruses as Blueprints for Nanoparticle Design 6

1.1.4 Methods to Quantify Cellular Uptake 9

1.1.5 Surface Engineering of Viral Vectors 11

1.1.6 Quantifying Viral Internalisation with Molecular Probes 14

1.2 Aims of research **15**

2. Chapter 2. General Methods ***18***

2.1 Materials **18**

2.1.1 Plasmid constructs and primers 18

2.1.2 Cell culture and experimental cell lines 18

2.2 Lentiviral Production **19**

2.2.1 Plasmid Design and Construction 19

2.2.2 Generation of lentivirus with 293FT cells 19

2.2.3 Concentrating and labelling of generated lentiviruses 20

2.2.4 Validation through SDS-PAGE 20

2.3 Characterisation of Lentivirus **21**

2.3.1 Viral Titre 21

2.3.2 Particle Sizing and Concentration Measurement 21

2.3.2 Degree of Labelling Studies 21

2.4 Internalisation Time Course Studies with Lentivirus **22**

2.4.1 Quenching Efficiency and Internalisation 22

2.4.2 Experimental Design and Flowchart 23

3. Chapter 3. Generation and Validation of Sensor Attached Lentivirus 24

Abstract 24

3.1 Conventional Click Chemistry Attachment of Direct Sensor 24

3.2 HaloTag Expression on Lentiviral Envelope Plasmid for Sensor Conjugation ... 27

3.2.1 Generation of mEmerald GFP Transfer Plasmid 30

3.2.2 Generation of HaloTag VSV-G Tag Envelope Plasmid 32

3.2.3 Assembly and Verification of Preliminary Lentiviral Production 33

3.2.4 Labelling Method Optimisation Post Lentiviral Transfection 34

3.3 Optimisation HaloTag Expression on Lentiviral Surface Membrane 36

Chapter Summary 38

4. Chapter 4. Characterisation and Degree of Labelling Studies 39

Abstract 39

4.1 Importance in Lentiviral Characterisation 39

4.2 Characterising HaloTag-VSVG Tag Lentivirus 40

4.2.1 Particle Size of HaloTag-VSVG Tag Lentiviruses using NTA 40

4.2.2 Functional Viral Titre vs. Total Particle Concentration 41

4.3 Characterising Halo-sCy5-TCO Internalisation Sensor on Lentiviruses 42

4.3.1 Optimising Sensor Activity Assay with Compensation Beads 42

4.3.2 Quenching Efficiency of Internalisation Sensor 45

Chapter Summary 47

5. Chapter 5. Uptake and Internalisation Studies 48

Abstract 48

5.1 Viral Uptake and Internalisation 48

5.1.1 Viral Internalisation Efficiency in HEK293 Cells 49

5.2 Correlating Number of Labelled Viral Particles with Transduction Efficiency 51

5.3 Future Impacts and Direction 54

Chapter Summary 55

6. Appendix 56

Appendix A 56

Appendix B 56

Appendix C **57**

Appendix D **58**

Appendix E **59**

7. References ***60***

Abstract

Recently there has been developments in nanoparticles as delivery systems to overcome limitations associated with traditional drug carriers. Nanoparticles can encapsulate drugs, proteins, or nucleic acids to limit potential degradation and improve upon issues such as poor solubility and off-target effects with specific targeting. Despite the significant improvements in the physicochemical properties of nanomaterials as novel delivery platforms, endocytosis is still regarded as the main uptake and internalisation mechanism. Even with controlled release and active targeting, the majority of the therapeutic cargo still becomes entrapped and degraded in the lysosomes, hindering efficient transport and delivery. Viruses are nanomaterials that surpasses many of the newer synthetic nanoparticles for biomedical applications, possessing great efficacy in cell interaction and crossing complex biological barriers. This thesis explores the different routes of nanoparticle uptake and endocytosis and attempts to address the limitations of current tools for observing internalisation as well as surface conjugation methods for viruses through the development and expression of HaloTag fusion protein and HaloTag ligand adaptor system on lentiviral surfaces.

Lentiviral vectors are a common method for many applications that require stable genetic modification of cells *in vitro* as they can effectively integrate their genetic payload into the chromosomal DNA of their host cell. These vectors are often produced with an alternative envelope protein in their lipid membrane, in particle vesicular stomatitis virus (the VSV-G protein). The VSV-G protein has been known for its broad tropism and binds to LDL receptor family members. This presents as a perfect platform to observe efficient viral internalisation with the use of internalisation tools.

Molecular sensors designed with triggerable fluorescence provides an opportunity to distinguish between surface bound and internalised materials and are often utilised with fluorescent markers. An internalisation sensor designed by Selby L. et al uses click chemistry to specifically quench extracellular signal, leaving the intracellular signal affected. However, the challenge lies with conjugating these sensors onto live viruses without affecting their delicate structures and interfere with carrier infectivity. More recently, genetically encodable adaptor systems have gained attention as a viable conjugation method, in particular HaloTag fusion protein and HaloTag ligand.

This thesis demonstrates the construction of HaloTag fusion protein expressed VSVG envelope plasmid as well as the conjugation of a molecular sensor designed for probing cellular internalisation onto the viral surface. The assembled lentiviruses with HaloTag expression were then efficiently labelled with the signal observed using flow cytometry and optimised with the use of compensation beads. Sensor and quenching activity were also observed to demonstrate effective functioning and ability to quantify cellular internalisation.

Internalisation of the labelled lentiviruses with HEK293 cells were observed and quantified without the sensor compromising viral viability and infectivity. Overall, this thesis presents the design, synthesis, and validation of method to probe viral internalisation *in vitro*. The conjugation method using the HaloTag adaptor system presents a facile way to label live viruses and provides an additional means to nanomaterial scientists and virologists to assist in the design of carriers for drug delivery and in our understanding of viral internalisation mechanisms.

Declaration

This thesis is an original work of my research and contains no material which has been accepted for the award of any other degree or diploma at any university or equivalent institution and that, to the best of my knowledge and belief, this thesis contains no material previously published or written by another person, except where due reference is made in the text of the thesis.

Signature:

Print Name:

Date:

Acknowledgements

To begin I would like to express my sincerest gratitude and thanks to the Johnston group. I am incredibly grateful to my supervisor Dr. Angus Johnston for his encouragement and support in my project and work. His leadership and dedication have made my time here truly enjoyable, and I am happy to have been part of a truly wonderful research team. I would like to extend a special thanks to our post-doctoral fellows Dr. Daniel Yuen, Dr. Niloufar Ansari and research assistant Moore Chen for their hardworking and tireless efforts in maintaining the lab and willingness to give up their time to share their knowledge with others.

From Monash University, I would like to thank Sandy Fung, Padmini Nanda and Cameron Nowell for lending their expertise in flow cytometry and research project staff Karen Drakatos, Karen McConalogue, Gabrielle Bright, James Ashman-Jones. I would also like to thank Assoc. Prof. Colin Pouton for sharing his knowledge with me. I am grateful to Dr. Orlagh Feeney for her wisdom and encouragement, it would have been even more challenging to finish this project without her help. I would also like to thank Jessica Huang, Yih Rue Ong, Joshua Rennick, Serena Teo, Lara Molle and Alina Lam for lending a helping hand and getting excited and frustrated with me about the successes and mishaps happening in the lab – I have thoroughly enjoyed the company of such passionate and like-minded scientists.

I would also like to thank my panel members Dr. Robert de Rose, Dr. John Quinn, and Dr. Nicholas Veldhuis for their involvement in my project and invaluable advice over the time of my enrolment. In addition, I would like to thank Laura Fitzgerald for her synthesis of the HaloTag internalisation sensor and quencher. I am extremely grateful to my partner Calvin Nuon for his constant love and companionship and thank him for believing in me. I would like to thank my parents William and Rose, and my brother Nicholas for their emotional support during this time. I am also appreciative of the continuous company and friendship provided by my cat Luna and dog Peanut.

Finally, I gratefully acknowledge Monash University and the ARC Centre of Excellence in Convergent Bio-Nano Science and Technology for their support and the opportunities they have provided throughout my Master's.

Abbreviations

/kb	per kilobase
%	percentage
°C	degree Celsius
µg	micrograms
µL	microlitre
µM	micromolar
ANOVA	Analysis of Variance
ARF1	ADP-ribosylation Factor 1 Protein
ATP	Adenosine Triphosphate
AUC	Area Under the Curve
CD34	Cluster of Differentiation 34
CDH	Cyclohexadienyl Dehydrogenase
CIN85	Cbl-interacting Protein of 85 kDa
CLIC	Clathrin-Independent Carrier
CME	Clathrin-coated pit Mediated Endocytosis
DLS	Dynamic Light Scattering
DMEM	Dulbecco's Modified Eagle Medium
DNA	Deoxyribonucleic Acid
DPBS	Dulbecco's Phosphate-Buffered Saline
EDTA	Ethylenediaminetetraacetic acid
EF1	Elongation Factor 1a
EGFR	Epidermal Growth Factor Receptor
ELISA	Enzyme Linked Immunosorbance Assay
EM	Electron Microscopy
FBS	Fetal Bovine Serum
FEME	Fast Endophilin-Mediated Endocytosis
GBF1	Golgi Brefeldin A Resistant Guanine Nucleotide Exchange Factor 1
GEEC	Glycosylphosphatidylinositol-anchored Protein Enriched Early Endocytic Compartment
GFP	Green fluorescent protein

GTP	Guanosine Triphosphate
HEK293	Human Embryonic Kidney 293 Cells
HEK293FT	Human Embryonic Kidney 293 Cells (Fast growing variant transfected with the SV40 T antigen)
HGFR	Hepatocyte Growth Factor Receptor
HIFI	High Fidelity
HIV	Human Immunodeficiency Virus
IRES	Internal Ribosome Entry Site
LDL	Low Density Lipoprotein
MCS	Multiple Cloning Sites
MFI	Mean Fluorescence Intensity
MOI	Multiplicity of Infection
MWCO	Molecular Weight Cut Off
NHS	N-hydroxyl-succinimidyl ester
NTA	Nanoparticle Tracking Analysis
PBS	Phosphate-Buffered Saline
PCR	Polymerase Chain Reaction
PEG	Polyethylene Glycol
PFA	Paraformaldehyde
PVDF	Polyvinylidene Fluoride
RNA	Ribonucleic Acid
rpm	Revolutions per Minute
RT	Reverse Transcriptase
RT-PCR	Real-time Polymerase Chain Reaction
SD	Standard Deviation
SDS PAGE	Sodium Dodecyl Sulphate–Polyacrylamide Gel Electrophoresis
SVT	Single Virus Tracking
TCO	Transcyclooctene
TU/mL	Transduction Units per Millilitres
VSV	Vesicular Stomatitis Virus
VSVG	Vesicular Stomatitis Virus Glycoprotein

Chapter 1. Introduction

1.1 General Introduction

1.1.1 Statement of the problem

Global health has significantly improved through the research field of nanomedicine – the holistic approach of engineering and functionalising nanoparticles to diagnose and deliver drugs to prevent and treat diseases using molecular tools in combination with traditional therapeutics (1). Nanoparticles come in various shapes, sizes, and materials, with the physicochemical properties of nanoparticles controlled to ensure the success of therapeutic delivery to a specific cell or tissues with increased stability and targeting (2, 3). These efforts include using pH sensitive (4, 5) materials that have been designed to assemble/disassemble in response to external stimuli, providing controlled and steady release of cargo, or the surface pegylation of nanoparticles to reduce unwanted uptake (6, 7) and so forth.

Upon administration, the solubility of an oral drug plays an important role in absorption and its bioavailability. Nanoparticles can be used to improve drug solubility by increasing the surface area and therefore dissolution rate of the therapeutics according to the Noyes-Whitney equation (8). The next benefit of nanoparticles includes specific targeting of drugs in the form of active or passive targeting. Passive targeting relies on blood circulation to drive the drug loaded nanoparticles to the target site by binding or affinity based on external factors such as pH and temperature. Active targeting involves moieties such as antibodies or peptides coupled to the drug delivery system to anchor them to the receptor structures expressed at the target site (9). Evidently nanoparticles can overcome barriers on drug release and distribution, most delivery systems face a bottleneck in regards to crossing the plasma membrane and delivering the therapeutic cargo to its active site (10). Small molecules, free peptides, and proteins can readily cross cell membranes while cellular uptake of nanoparticles involve highly regulated mechanisms with complex biomolecular interactions involving endocytosis (11). After being internalised, the next hurdle nanoparticles face is endosomal encapsulation, which they must escape or end up being transferred to the lysosomes and degraded or excreted out of the cells. Overcoming this, nanoparticles will then be able to diffuse and localise within the cytoplasm, and be able to finally deliver its payload (12).

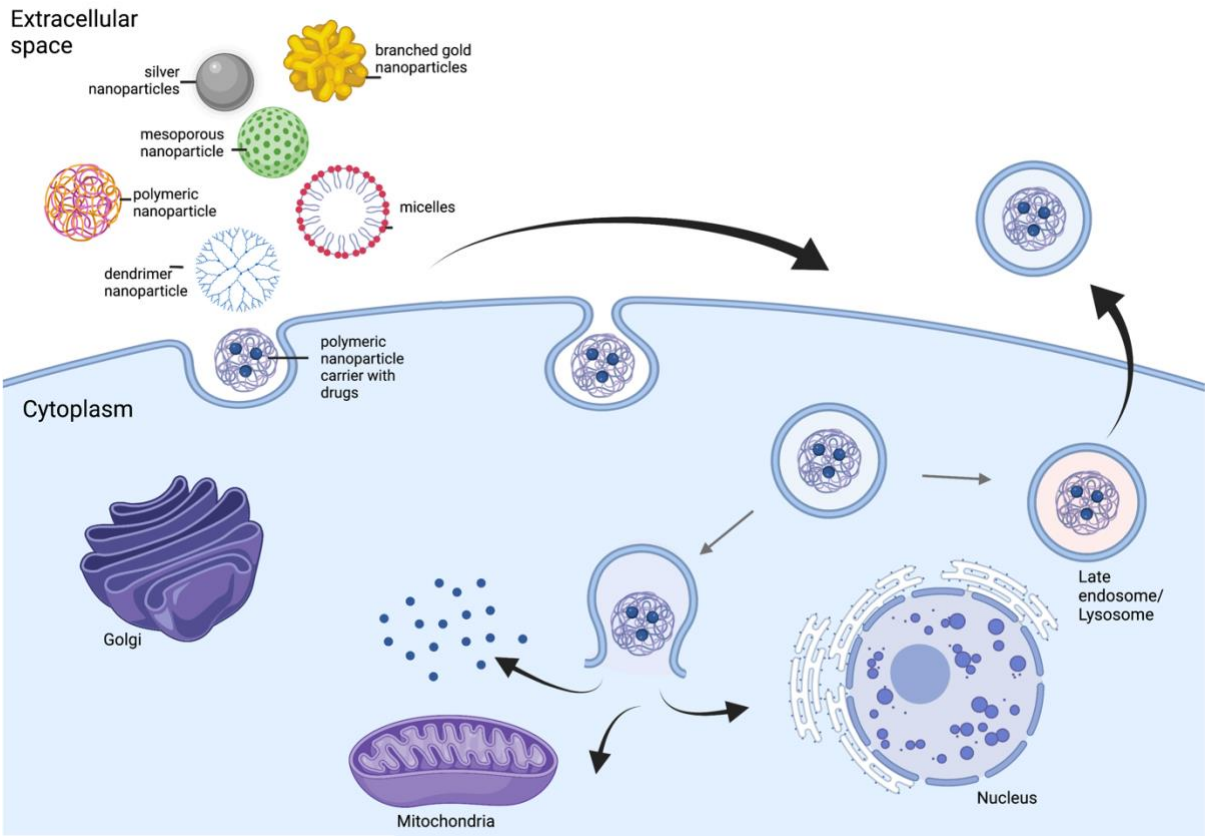

Figure 1-1 ***Overview of the journey of nanoparticles to deliver its therapeutic payload.*** *Adapted from Donahue N. et al, the journey of nanoparticles to its destination not only relies on the interactions at cellular level, but also at a subcellular level once internalised. After being internalised, nanoparticles may be able to escape to its specific site of action, recycled to the cell surface, or sent to the late endosome and lysosomes where it will be degraded. Figure designed in Biorender.com.*

As a consequence, the fate of therapeutic payloads (i.e., contrast agents, drugs, genes) to the cytosol, nucleus, or other specific site of action are ultimately linked to the capacity of nanoparticles to enter the cell, which are governed by multiple endocytic pathways (13, 14). While nano-bio interactions are equally important in the targeting and delivery to the specific subset of cells, endocytosis is recognized as the critical cellular processes that governs the entry and delivery of any foreign material, including nanoparticles (15). Therefore, an understanding of nanoparticle uptake and internalisation mechanisms is important for the development of efficient drug delivery systems.

1.1.2 Nanoparticle Internalisation Pathways

This section will extensively follow the review article by Rennick J. et al (2021) in describing current view of endocytosis and the different endocytic pathways.

Understanding the mechanisms by which nanoparticles can be internalised into cells is important for several reasons. First, the physical properties (for example size) of the

nanoparticles govern the mechanisms that mediate the uptake of the particle. Second, the rate of nanoparticle uptake is largely dependent on the internalisation mechanism. Finally, not all cells possess the same internalisation machinery; the same nanoparticle may be internalised by different mechanisms by different cell types (13).

Nanoparticles can enter the cell by two main endocytic mechanisms – phagocytosis (cell eating) or pinocytosis (cell drinking). Recent attempts for further classification have been made but based on the complexity that exists with the mechanisms that involved multiple factors, it can be simplified and distinguished as five major types of endocytosis: *(1)* clathrin-coated pit mediated endocytosis (CME; clathrin and dynamin dependent), *(2)* fast endophilin-mediated endocytosis (FEME, a clathrin-independent but dynamin-dependent pathway for rapid ligand-driven endocytosis of specific membrane proteins), *(3)* clathrin-independent carrier (CLIC)/ glycosylphosphatidylinositol-anchored protein enriched early endocytic compartment (GEEC) endocytosis (clathrin and dynamin independent), *(4)* macropinocytosis, and *(5)* phagocytosis (Figure 1-2).

Caveolae represent a sixth pathway, which in theory can also contribute to endocytic uptake. While caveolae can bud from the plasma membrane, few if any cargoes are dependent on caveolae for their uptake (13).

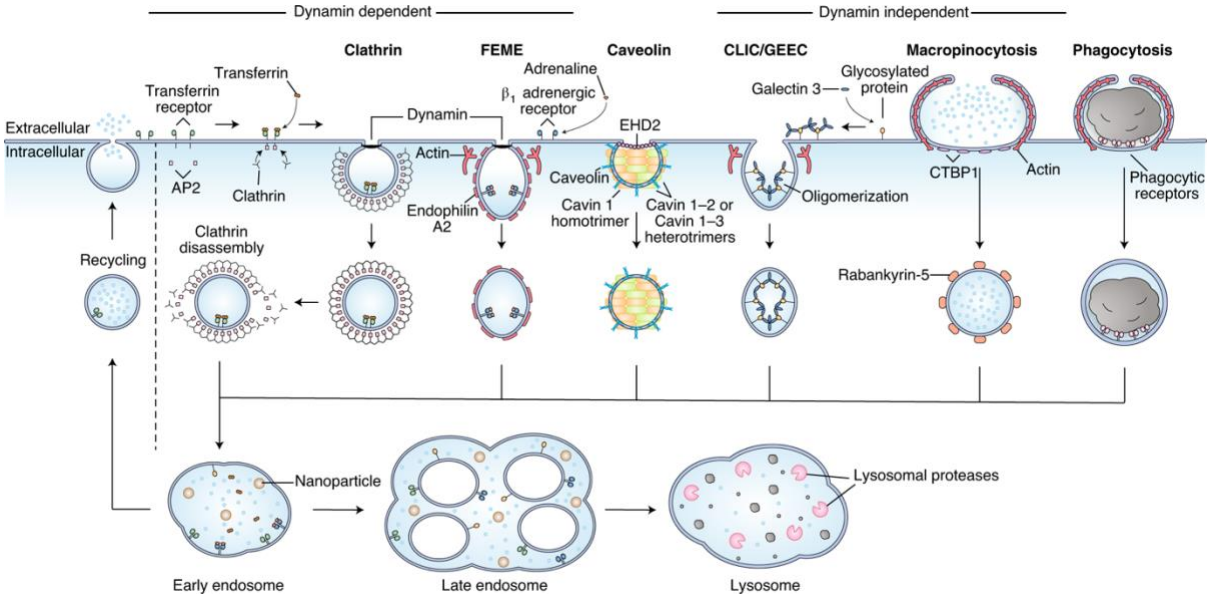

Figure 1-2 ***Endocytic pathways of nanoparticles into cells as described by Rennick J et al.*** *The adaptor complex, AP2, initiates the formation of clathrin coated pits and is the main driving force for CME. Endophilin A2 recruitment and actin polymerisation regulates FEME by triggering ligand-receptor interactions. Dynamin is required for both CME and FEME by facilitating membrane scission and involves cytoplasmic machinery through the interactions of the intracellular domains of cell surface receptors. Caveolin and cavin proteins are responsible for caveolae formation by forming Cavin homo- or hetero-trimers. Accessory protein Eps15 homology domain-containing 2 (EHD2) stabilizes the neck of vesicle to regulate endocytosis. CLIC/GEEC endocytosis is shown to*

be a continuous endocytic process that is independent of clathrin and dynamin but also receptor-ligand interactions. Carrier formation and cargo incorporation is mainly driven by extracellular galectin proteins (not shown) that co-cluster glycoproteins and glycolipids. Macropinocytosis involves the uptake of large volumes of fluid that requires stimulation that is controlled by actin polymerisation and C-terminal-binding protein 1 (CTBP1). Phagocytosis is also triggered by actin polymerisation after a binding event at the cell surface occurs, tightly forming a vesicle around the bound material. Following any endocytosis events, these pathways undergo sorting after merging into early endosomes, and may be sent back to the surface or onwards to the late endosome and lysosome (13).

1.1.2.1 Phagocytosis

Phagocytosis is an important element of cells in the innate immune system. Phagocytic cells (collectively known as phagocytes) such as macrophages, monocytes and dendritic cells engulf invading microorganisms and foreign material >500 nm in diameter (16). Immunoglobulins or other complement proteins are adsorbed onto the nanoparticle's surface, resulting in nanoparticles being opsonized and recognized by these phagocytes via specific ligand-receptor interactions (17). Phagosomes that pinch off inwardly are then created by fusion of cup-shaped protrusions and the plasma membrane of phagocytes, enclosing these nanoparticles and preferentially accumulating in the reticuloendothelial organs, e.g. liver and spleen (18).

1.1.2.2 Macropinocytosis

Macropinocytosis is characterised by actin-dependent formation of large-sized (200 nm – 5 µM) membrane protrusions. It is a unique process that occurs in almost all cell types, internalising nanoparticles and dissolved solutes and molecules from the extracellular fluid into endocytic vesicles. Macropinocytosis is distinct to other internalisation routes as it is a non-selective pathway that does not rely on the cargo binding to specific cellular receptors. Macropinosomes are also heterogeneous in size and much larger than other endocytic structures with no known structural proteins (19). Macropinocytosis presents a universal route into much broader range of cell types and may be important in the internalisation of nanoparticles that would not be possible via other endocytic pathways.

1.1.2.3 Clathrin-mediated endocytosis (CME)

Clathrin-mediated endocytosis is the major pathway for receptor endocytosis and contributes to over 95% of endocytic flux, assisted by an adaptor protein complex (20, 21). It serves as the main mechanism for nutrient uptake (e.g., uptake of iron via transferrin or cholesterol via low density lipoproteins) in mammalian cells and is responsible for efficient receptor signalling. A clathrin-coated pit is a highly dynamic system involving a multitude of interactions that forms a pit within 30-120 s of ligand

binding (22). The pit rapidly invaginates to form a clathrin-coated vesicle, which pinches off the plasma membrane through the activity of dynamin, a large mechanical GTPase. These smaller vesicles can only internalise nanoparticles with an average diameter of ~100 nm (22). With the distinct morphology of the clathrin-coated pit, this pathway has been extensively characterised, facilitating well research cargoes that are completely dependent on this pathway for uptake.

1.1.2.4 Clathrin-independent/dynamin-dependent endocytosis, FEME

FEME has recently emerged as an important pathway for rapid endocytosis of specific transmembrane receptors, important in growth factor signalling and in cell migration (23). The FEME pathway has several unique features that distinguish it from other pathways. First, the pathway is clathrin independent but dynamin dependent. Second, the formation of endocytic carriers is induced upon ligand binding to specific receptors. FEME relies on interactions between the SH3 domain of endophilin and cognate receptors (e.g., G-protein-coupled receptors) or indirect association through intermediate proteins such as CIN85 and CB1 (for EGFR and HGFR). Formation of FEME carriers is extremely rapid (<10 s), is dependent on the pre-enrichment of endophilin at the membrane and leads to the formation of tubular carriers, which are 60-80 nm in diameter and several hundred nanometres in length (23).

1.1.2.5 Clathrin-independent/dynamin-independent endocytosis, CLIC/GEEC

CLICs are involved in a distinct endocytic pathway, independent of dynamin or clathrin, which has been shown to be a high-capacity pathway in mammalian cultured cells and is also conserved in *Drosophila (24, 25)*. This pathway, termed CLIC/GEEC endocytosis, shares some features with the FEME pathway, as they both localise to the leading edge of migrating cells and involve tubular and ring-shaped pleomorphic carriers (ranging in diameter and length). However unlike FEME, which is stimulated by specific ligand-receptor interactions, CLIC/GEEC endocytosis is a constitutive pathway that mediates the uptake of cargoes that are different from those using the FEME pathway (23). The CLICs mature in tubular GEECs, and the pathway is regulated by ARF1/GBF1, the actin regulatory complex Arp2/3 and the small GTPase Cdc42 (26).

1.1.2.6 Caveolae: limited evidence for nanoparticle uptake

An extensive literature links caveolae to endocytosis. Caveolin dependent endocytosis is regulated by dynamin and operates through caveolae, which are formed by caveolins and cavins (27). Being one of the earlier plasma membrane structures observed through electron microscopy, caveolae are coated, flask-shaped invaginations, implicated in a variety of cellular processes, e.g. transcellular transport, membrane repair, and mechanotransduction (20). However, the role of caveolae in the endocytic processes is not clear despite the dogma that has developed in some research fields. Not only are there contradictory studies in which genetic knockout of caveolar components observed have not generally shown a dependence of caveolae for endocytic uptake in any system (28, 29) but there is also the question of physical accommodation of cargo internalised. The interior of caveolae is generally described around 50 nm in diameter, representing a small space for a relatively small cargo. Significant modifications would have needed to be made in order to accommodate materials greater than this diameter and should not be considered caveolae (13). With the limited evidence for nanoparticle uptake, some reservations should be made until this pathway have been clearly distinguished and characterised.

Despite the different endocytic routes for cellular uptake, the majority of nanoparticles drug delivery systems become trapped in the early endosomes are subsequently trafficked into late endosomes and lysosomes where they are degraded by enzymes (14). This results in a rate limiting step. In order to achieve effective therapeutic delivery, facilitating endosomal escape and ensuring cytosolic delivery of nanoparticles becomes one of the key aspects in efficient drug delivery (30).

1.1.3 Viruses as Blueprints for Nanoparticle Design

Viruses represent a group of robust and natural nanomaterial for the efficient transport of genetic information by sophisticated mechanisms, inspiring the design of many nano-architectures with successful drug and gene delivery (31). Exhibiting characteristics significant to drug design and delivery, viruses exhibit an intrinsic ability to avoid immune system recognition while also having the ultimate target cell specificity with use of a consecutive multistep process for cell identification. Adenoviruses, retroviruses, and lentiviruses are all viral vectors that have observed to have great efficacy in treating of adenosine deaminase deficiency and X-inked severe combined immunodeficiency. Despite their versatility and effectiveness in cargo

delivery, viruses are pathogenic in nature and concerns regarding their safety profile remains a substantial issue. Viral size and payload limitations further hinders the possible applications of viruses as therapeutic functions despite additional efforts in vector engineering and modification of their viral surfaces (32, 33).

Virus-like particles and virosomes were created to avoid the issue of introducing viral genetic material while being able to take advantage and gain the benefits of viral properties. Virus-like particles are particles that self-assemble and mimics the viral capsid structure, while virosomes resemble liposomes whose phospholipid bilayer are modified to incorporate the surface glycoproteins of actual viruses (34). Both structures provide promising potential in drug delivery applications as it averts the risk of transferring viral genetic material and have increased capacity for various payloads (e.g., small molecule therapeutics, antibodies, proteins, or siRNA) with their hollow structures. By retaining some virus-like qualities, targeted delivery can still be achieved through efficient cellular entry and escape from endosomal entrapment (33).

Aside from mimicking viral architecture and structures, other viral features become an area of interest for surface modifications of nanoparticles. Enveloped lentiviruses have specialised glycoproteins that hijack the endocytic pathways of host cells. Through the fusion of the envelope protein expressed on the viral membrane with the host cell membrane, this allows them to effectively enter host cells without being prematurely recycled or degraded (35). By copying the rough surfaces of enveloped viruses, functionalised nanoparticles have increased likelihood of association and cellular uptake with higher retention of payloads, resulting in a more effective carrier for siRNA delivery (33, 36).

Viruses pseudotyped with the vesicular stomatitis virus envelope glycoprotein (VSV-G) presents an opportunity to further observe and evaluate internalisation and trafficking within cells. VSV-G pseudotyped vectors have demonstrated good transduction efficiency in a wide host range and are more uniformly infectious with higher titres while providing purification advantages due to the increased stability of the vector particle (37). This presents a useful approach in determining the driving force for surface modifications in nanoparticles and facilitate a model for constructing carriers that target sub-cellular components to deliver therapeutic cargo with a higher therapeutic efficacy.

Methods that rely on post-entry parameters, such as replication or the expression of a reporter gene can be very limiting in better understanding viral entry (38). By measuring fluorescence output to detect replication-dependent viral protein, reporter-fusion protein expression, viral entry and replication processes are not clearly distinguished and may not be helpful when determining the properties to improve internalisation in nanoparticle applications.

Studying virus entry directly, i.e., in a virus replication-independent manner, has proven to be difficult, certainly when using low, physiologically relevant amounts of viral particles (39). Radioactive labelling of structural viral components, the use of organic dyes, fluorescent protein and electron microscopy of infected cells were among the variety of methods that have been applied. However, chemical labelling of viruses often resulted in compromised infectivity, and viral fusion and internalisation are not observed directly even with visual insight into virus entry owing to the various stages of the entry.

Single virus tracking (SVT) techniques have also been developed over the last decade to detect viral fusion in real-time. This technique visualises individual viral particles in real time and *in situ* dynamics of viral processes in live cells, avoiding ensemble averaging to analyse dynamic behaviours of single viruses in their native, complex surroundings. Although this approach is highly sensitive, it only provides an estimate of viral behaviour based on the characterisation of isolated viral particles, which might not accurately predict and characterise the bulk efficacy of viral populations. Since single virus tracking also requires labelling the viral components and limitations can arise with the types and size of labels on top of the risk of inhibiting functionality or even assembly of the virus. Organic dyes, fluorescent proteins, and nanoparticles are commonly used for labelling viral structures, each with their own sets of advantages and drawbacks (40-42).

Given the range of techniques described above, the knowledge of uptake and internalisation kinetics of viruses are often limited and sometimes conflicted. Thus, this is a poorly understood aspect of virology with no single method being sufficient to determine all the details of viral assembly, replication, entry, and transduction.

1.1.4 Methods to Quantify Cellular Uptake

The different properties required for efficient internalisation with viruses or nanoparticles alike be it the effects of size or shape, are affected by the ability to determine and measure such uptake. The techniques and assays used to quantify internalisation are important from a mechanistic standpoint as the different endocytic pathways involved in nanoparticle uptake can be addressed. In addition, many of these analytical approaches have also been made to distinguish association from uptake and internalisation.

Herein, we provide an overview of the techniques currently used to quantify internalization as described by Fitzgerald L et al. (Figure 1-3).

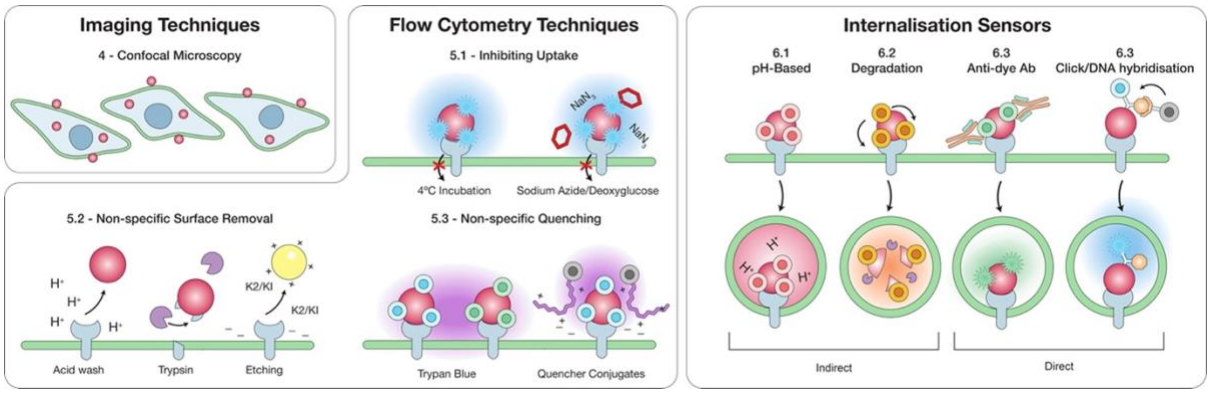

Figure 1-3 ***Summary of techniques for determining uptake, taken from Fitzgerald et al (43)****. Techniques are categorised into imaging, quantitative flow cytometry, and internalisation sensors. Direct visualisation of nanoparticle internalisation can be observed using microscopy while flow cytometry represents a more quantitative approach. Internalisation sensors can be direct or indirect, requiring distinction from surface bound and internalised material.*

Fluorescence based methods and imaging techniques, specifically using microscopy or flow cytometry are amongst the most common for determining uptake. Both methods heavily rely on labelling nanoparticles with fluorescent markers, dyes, or molecular sensors, such as pH-sensitive or DNA hybridized sensors, and anti-dye antibodies.

While confocal microscopy provides greater resolution at ~250 nm (44) to visualise intracellular distribution, analysis of the generated images are still subjected to individual interpretation, with the roughness of the cell membrane adding to the uncertainty whether the material is bound or internalised. Additionally, a single slice is inadequate for quantifying internalisation as endosomes are unevenly distributed throughout the cell (45) and samples may vary across throughout collection. Super-resolution microscopy may improve the resolution to as low as < 50 nm but is also

time-consuming and requires a complete 3D section of the cells for quantification. High resolution transmission X-ray microscopy (TXM) has also been used to study internalisation, but it is heavily reliant on synchrotron-based source of X-ray, access to the required facilities may be difficult and not practical for frequent studies (43, 46).

While microscopy allows visualisation of nanoparticle interactions with cells, the combination of molecular sensors with the use of flow cytometry is more amenable to quantifying internalisation. The rapid acquisition in flow cytometry allows for a much higher throughput, being capable of acquiring data at a rate of thousands of cells per second, generating much larger sample sizes for more robust statistical analysis (47). Because it gives no information about the location of the fluorescent signal, flow cytometry relies on the distinction of fluorescent signal from the surface bound and internalised nanoparticles. Several methods have been developed to non-discriminately and physically detach proteins or nanoparticles from cell membrane.

First introduced in the early 1980s, the acid wash method can be used to dissociate surface-bound material from the cell by exploiting the natural dissociation of the ligand-receptor complex. However, the acid-wash treatment is not completely efficient in surface protein removal, as demonstrated with pH-dependent receptor binding of transferrin (48), severely limiting the use of this method in the study of nanoparticle internalisation. Particles may remain on the surface if the particle binding is not pH sensitive or binds strongly to multiple regions of the cell surface. Potential toxicity from the acid-wash treatment can also affect cell viability and compromise overall acquisition of cells for analysing on flow cytometry (49, 50).

The use of proteases, such as trypsin, are also a common technique in the removal of material bound to receptors. Cleaving at the carboxyl side of both lysine and arginine residues, trypsin is able to digest the cell surface proteins (51, 52). However, this method is also unreliable as a method to remove surface bound nanoparticles as it can only remove the material if they are indeed bound to proteins. Membrane impermeable dye trypan blue can also be used to non-specifically remove remaining fluorescence on the cell surface (53, 54). While routinely used to establish cell viability (55), trypan blue has been used in flow cytometry and confocal microscopy to remove the fluorescence signal on the outside of the cell (56, 57). However, trypan blue may cause an increase in autofluorescence as it can bind to certain proteins and non-

specifically quench other surface markers needed for immunophenotyping, potentially compromising the signal to noise ratio (58).

Internalisation sensors were designed and developed to accommodate the range and diversity of therapeutic targets that were not suited for acid-washing or trypsin cleavage. Based on the review Fitzgerald et al. published, an ideal internalisation sensor should be single fluorophore-specific; be easily attachable to a nanoparticle or protein; be multiple analysis technique-compatible, for example, compatible for both flow cytometry and fluorescent microscopy; and preferentially not require any further processing after nanoparticle-cell incubation (43).

Recent developments of molecular sensors include pH-sensitive sensors that increases in fluorescence intensity with the shifts in pH (59, 60) or emit at different wavelengths depending on the protonation state of the fluorophore (61), degradation sensors that degrade once internalised and regain fluorescence when treated with a protease and sodium dodecyl sulphate (62), and direct sensors that enables signal detection regardless of location and duration after the nanoparticle has been internalised (63). Despite the varied techniques of the sensors, majority of them presents drawbacks to their uses, with the pH-sensitive sensors only useful for quantifying internalisation into acidic endo/lysosomal compartments and requiring dual-labelling whereas degradation sensors are inappropriate for materials that do not degrade or recycled, such as transferrin (64, 65), and are dependent on the properties of the material and the cell type.

1.1.5 Surface Engineering of Viral Vectors

Lentiviruses have been widely used in both therapeutic and basic biological applications due to their ability to integrate genomes of both dividing and non-dividing cells, mediating stable and long-term transgene expression (66). Viral surface functionalisation is required for the development of both lentiviral applications and oftentimes these techniques need to efficient and flexible. Controlling the viral surface environment would not only be beneficial in the manufacturing aspects of viral production but can also enhance the functionality and utility of the vectors for further research. Alternative viral surface modification can be broadly separated into three categories: (i) direct covalent modification, (ii) the use of membrane-binding moieties, and (iii) the use of adaptor systems. These categories may also overlap, such as the

use of transfection or a chemical covalent modification to deliver an adaptor site. Specific genetic engineering and modification of these surfaces via viral vectors can also be considered before the viruses are transfected. Nonetheless, creating an adaptor site for molecular sensors using viral vectors alone would also be very technically challenging and unpredictable in nature (67).

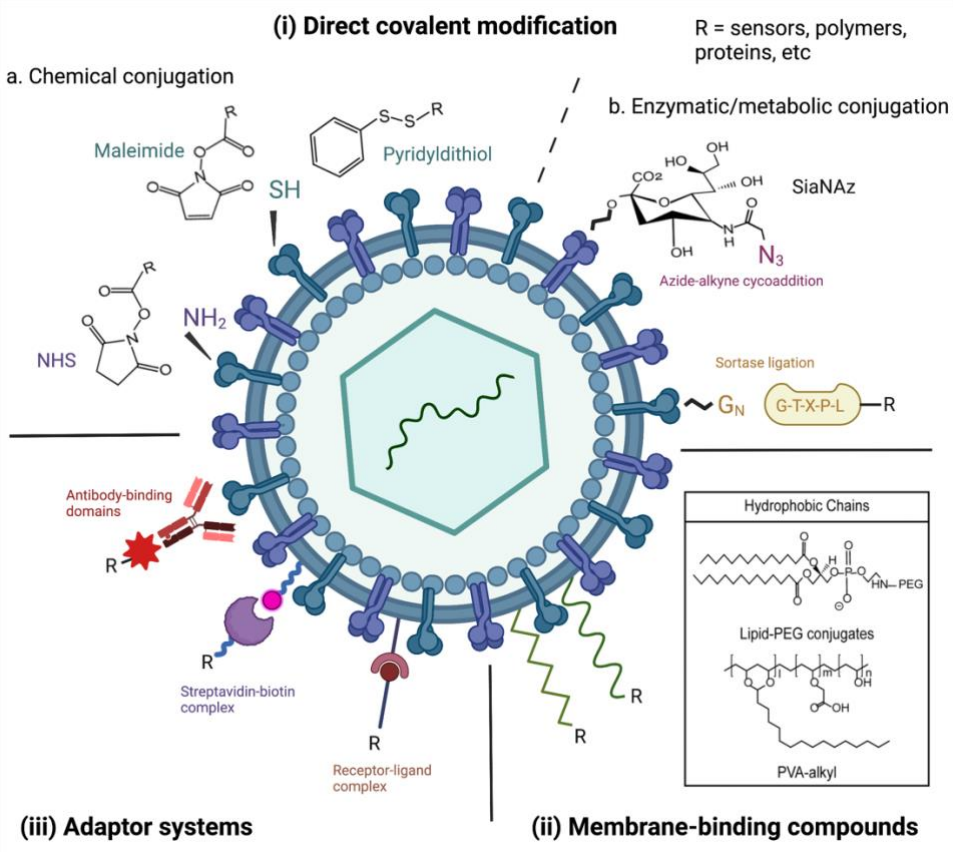

Figure 1-4 ***Different viral surface engineering techniques, adapted from D. Lee et al (68)****. (i) Incorporation of cross-linkers, such as NHS, Maleimide, or pyridyldithiol, allows viral surface conjugation with sensors through chemical covalent conjugation. Cell metabolism of unnatural sugar and enzymatic reactions can also be exploited to attach these sensors on the cell surface. (ii) Lipid-conjugated sensors or polymers with long alkyl chains can be embedded into the viral membrane through hydrophobic interaction. (iii) Adaptor systems include integrated biotin-acceptor peptides that can be coupled to an avidin-containing sensor. Antibody-binding domains that is genetically incorporated can also be used to couple antibody containing sensors to the vector. Abbreviations: NHS: N-hydroxyl-succinimidyl ester; SiaNAz: N-azidoacetyl sialic acid; PEG: Poly(ethylene glycol); PVA: Poly(vinyl alcohol). Figure designed in Biorender.com.*

(i) *Direct covalent modification.* A covalent conjugation approach uses chemical linkers that react with specific chemical groups to be conjugated, such as using N-(3-Dimethylaminopropyl)-N’-ethylcarbodiimide/N-Hydroxysulfosuccinimide (EDC/Sulfo-NHS) chemistry to mediate the formation of a an amide bond and act as a zero-length crosslinker (69). In theory, chemical covalent modification of the viral surface structure has better targeting for compounds on the viral surface and allows for a more

directed and specific reaction. However, this strategy applies more to naked viruses without an enveloped surface such as adenoviruses and adeno-associated viruses, which are inherently more chemically stable (70). Conversely, direct covalent modification has not been commonly attempted on enveloped viruses since viral infectivity is often adversely impacted (71). Recently, this has been circumvented by using biological chemistry. For example, bio-orthogonal labelling methods that were originally established in bacteria have appeared to have great potential for novel types of viral surface modification. This provides more options for the modification of viral proteins, but the method is still technically challenging, and the covalent nature of the association could lower the efficiency of the conjugation (72). In most cases however, direct protein modification is still relatively difficult since any chemical procedures would result in protein interference and potentially affect its stability and function.

(ii) *Membrane-binding compounds.* Retroviruses and lentiviruses are covered by a lipid bilayer derived from the host cell membrane carried over during viral budding, incorporating viral envelope glycoproteins that recognise receptors on host cells (73). While this allows for the introduction of molecules with an affinity or tropism for lipid structures to modify enveloped viral vectors, it can compromise virus biology when attachment is located near important interaction sites due to steric hindrance as well as issues with long term stability (74, 75). Compared to direct chemical modifications and the use of membrane-bound adaptors, there is usually no requirement for ‘activation’ with compounds that have high membrane-binding affinities. This allows for increased biocompatibility and passive retargeting but is still limited to the fragility of the viral envelope structures since they are prone to chemical and physical damage and the change in structural integrity or even differences in the surface potential could impact on viral infectivity (76).

(iii) *Adaptor systems.* Surface modification may be achieved by using novel molecular adaptor systems (77). Natural ligands, small peptide motifs, or even dendrimer polymers can function as molecular adaptors to bind targeting groups on the surface of viral vectors (78). Such adaptors may also be used as linkage to a third element, such as binding small molecules to the viral vectors. These systems are mainly used as targeting strategies

in gene therapy but present a viable option for surface modification (79). While this system demonstrates the ability to conjugate a wide scope of substrates, several limitations include requiring strong affinity and binding to the receptors. It also requires multistep procedures and the *in vivo* stability of these complexes are still debatable (67).

1.1.6 Quantifying Viral Internalisation with Molecular Probes

The majority of these techniques mentioned have significant limitations – microscopy techniques are relatively low throughput and requires discretion in determining internalised material while flow cytometry requires the use of molecular sensors to association vs. internalisation. Acid-wash and trypsin digest techniques are ineffective in removing surface bound material and is affected by the type of receptor or ligand binding. Non-specific fluorescence quenching limits the use of phenotyping antibodies in mixed cell populations and introduces other artefacts. Environmental sensors are only useful when detecting internalised materials within acidic compartments and requires dual labelling of the materials to separate uptake and internalisation.

The use of specific internalisation sensors that specifically quench the fluorescence of material on the surface of cells can significantly simplify the quantification of nanoparticle uptake. One current and promising example is a modified and upgraded molecular sensor system that has been developed by Fitzgerald et al. This sensor forms attachments to the material using a trans-cyclooctene (TCO) conjugated to a Cy5 fluorophore via a carboxylic acid group (sCy5-TCO), while a compatible quencher attached to a tetrazine group (sQSY-Tet) is used to remove the fluorescence signal remaining on the cell surface. This sensor can then be attached to viruses and incubated with cells for a desired length of time. Then the cells are cooled to 4°C, limiting cellular uptake and endocytosis and addition of the quencher allows the removal of the remaining surface bound signal, but not the internalised material.

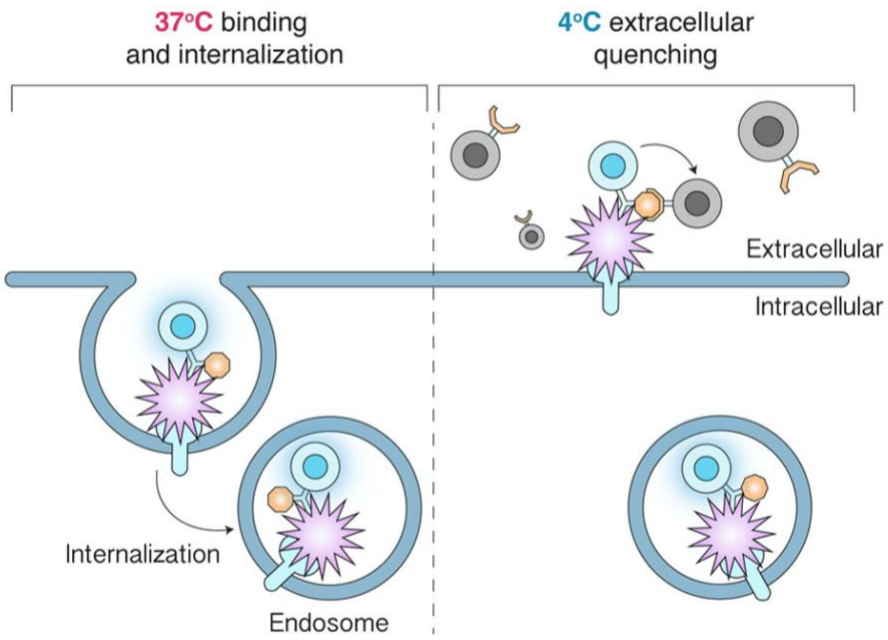

Figure 1-5 ***Quenching of extracellular signal from internalisation sensor at 4°C.*** *Schematic diagram of binding and internalisation of the protein or material into cells at 37°C, uptake is halted by bringing the temperature down to 4°C. The fluorescence of any material on the surface is removed selectively by adding the quencher of the sensor, leaving the intracellular signal unaffected (80).*

However, given the factors and properties required in observing uptake and internalisation, existing assays and techniques not only rely on the types of sensors or probes used, it is also crucial to optimise the conjugation approach in applying these sensors.

1.2 Aims of research

The proposed hypothesis for this thesis is the use of the fusion protein, HaloTag and the HaloTag ligand, to provide more efficient labelling and functionalising of lentiviruses without compromising infectivity and integrity of the structures. The versatility of this approach can also be applied for the use of other direct sensors as well as other biocarriers and drug delivery systems.

The aim of this research can be achieved through developing a facile method to produce lentiviral systems with the correct expression of the HaloTag fusion protein on the viral surface along with subsequent characterisation and profiling of the viruses made. Basic characterisation can be made using dynamic light scattering and the infectivity of the viruses can be tested with the use of a GFP reporter gene. The efficiency and degree of labelling of the internalisation sensors with the viruses can also be observed via flow cytometry. To this end, we hope to observe the internalisation kinetics of VSVG pseudotyped lentivirus over a duration of time as a

proof of concept to further support the use of direct sensors in understanding viral internalisation.

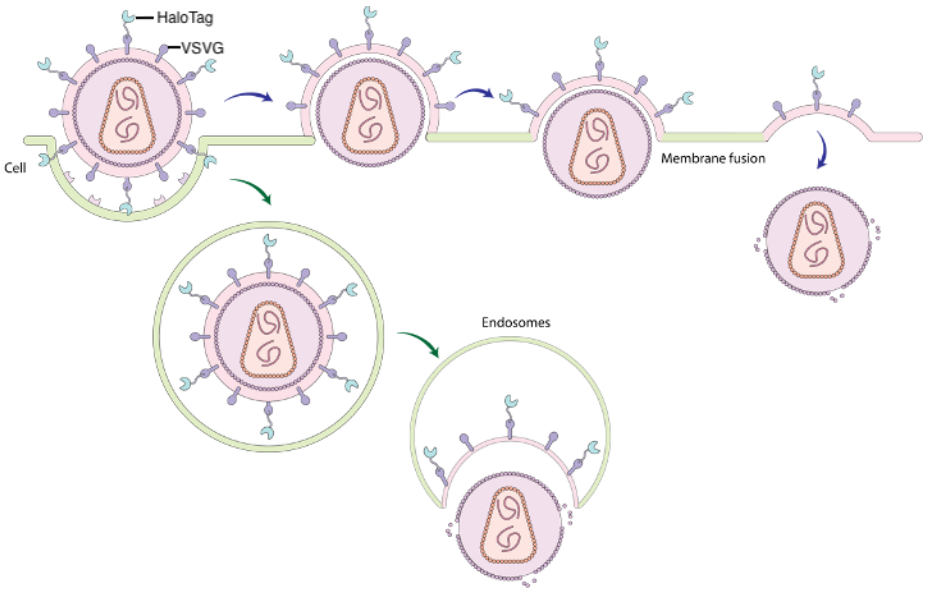

Figure 1-6 ***Possible internalisation pathways of HaloTag-VSVG-pseudotyped lentiviruses.*** *Schematic representation of modified VSVG lentivirus with HaloTag protein expressed on the viral membrane associating with the cell membrane, resulting in possible membrane fusion and subsequent internalisation, or endocytosed completely into an endosomal compartment that can also become fused with the viral membrane.*

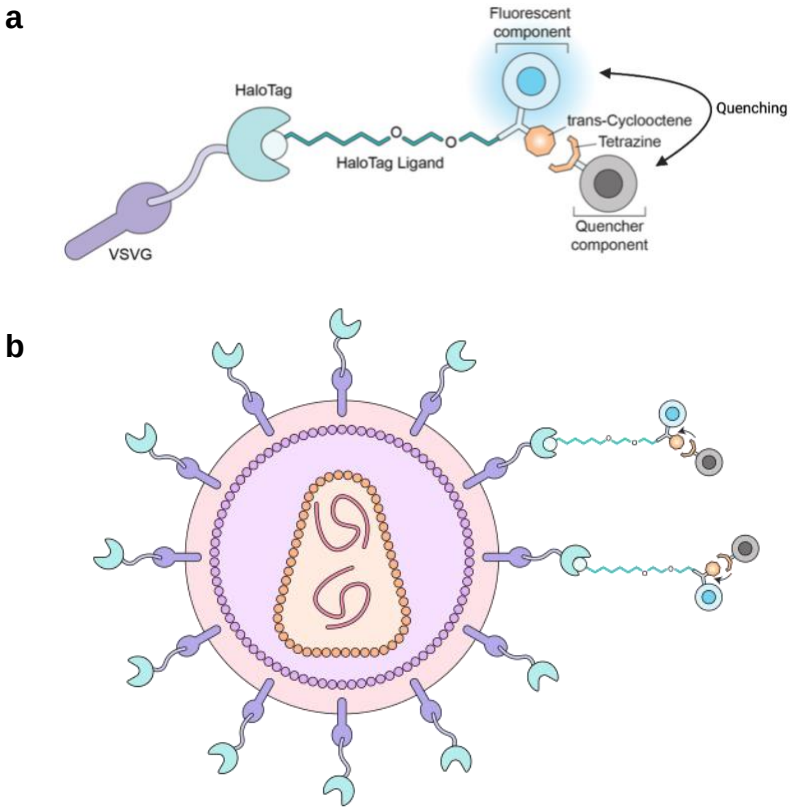

Figure 1-7 ***Using HaloTag ligand to attach an internalisation sensor. (a)*** *Schematic representation of functionalised Halotag-VSVG on pseudotyped lentivirus to observe viral internalisation. The Halotag ligand can be conjugated to the click component of the internalisation sensor developed by Fitzgerald et al (Halo-sCy5-TCO) and also be able to bind to the Halotag protein on the VSVG protein. The tetrazine group on the quencher component*

can react to the sensor and effectively quench any fluorescent signal remaining on the surface (data unpublished). ***(b)*** *Due to the versatility of the Halotag ligand, the internalisation sensor can be labelled on the Halotag protein expressed on the surface VSVG protein. This would be able to observe internalisation and uptake of VSVG-pseudotyped lentivirus, probing the efficient delivery of virions and nanomedicine alike (data unpublished).*

Since the size of most viruses is below the resolution threshold of common flow cytometers, it is challenging to measure the fluorescence intensity of a single virus particle (81). To overcome this, we will develop a high throughput approach to capture a known number of viral particles onto a larger particle that will enable us to accurately measure the fluorescent signal from an individual virus.

With the underlying aim of this research outlined in this thesis, more insight into nanoparticle interaction with cells can be gained through quantifying and distinguishing uptake and internalisation using a direct sensor. By demonstrating the efficacy of this sensor even with a complex viral system, this sets a standard of consistency for methods across the multiple techniques explored and thus will allow us to create better and improved drug delivery systems.

Chapter 2. General Methods

2.1 Materials

2.1.1 Plasmid constructs and primers

Plasmid pCDH-EF1α-MCS-IRES-Puro was purchased from System Biosciences (Palo Alto, USA) while plasmid mEmerald-Rab5a-7 was a gift from Michael Davidson (RRID: Addgene_54243). HaloTag-VSVG-tag sequences were purchased as DNA oligonucleotides from Integrated DNA Technologies (IDT) and inserted into pMD2.g lentiviral envelope plasmid, a gift from Didier Trono (RRID: Addgene 12259). All plasmids contain ampicillin resistance cassettes. Restriction enzymes were purchased from New England Biolabs (Massachusetts, USA). Phusion High Fidelity DNA polymerase and NEB 5-alpha competent *E.coli* bacteria were also purchased from New England Biolabs (Catalog no.M0531L and C29871 respectively). GoTaq PCR master mix, Wizard SV miniprep DNA purification system, and Wizard SV Gel and PCR clean-up system was purchased from Promega (Catalog no. M7122, A9282, and A1470 respectively; Wisconsin, USA).

2.1.2 Cell culture and experimental cell lines

Dulbecco's Modified Eagle Medium (DMEM) (4.5g/L glucose, 110 mg/L sodium pyruvate, no glutamine), 100xGlutaMAX supplement, Dulbecco's Phosphate-buffered saline (DPBS, no calcium, no magnesium) and TrypLE were purchased from Thermo Fisher Scientific.

Human embryonic kidney cells (HEK293, ATCC Cat# CRL-1573, RRID: CVCL 0045) and fast growing variant HEK293FT (RRID: CVCL_6911) were cultured in DMEM supplemented with 10% fetal bovine serum (FBS), 1x GlutaMAX and 100 units/mL of streptomycin and penicillin, with addition of 500 μg/mL for the fast-growing variant. Both cell lines were maintained at 37°C in a 5% CO_2 atmosphere, and sub-cultured every 2-4 days when 70-90% confluency was reached.

2.2 Lentiviral Production

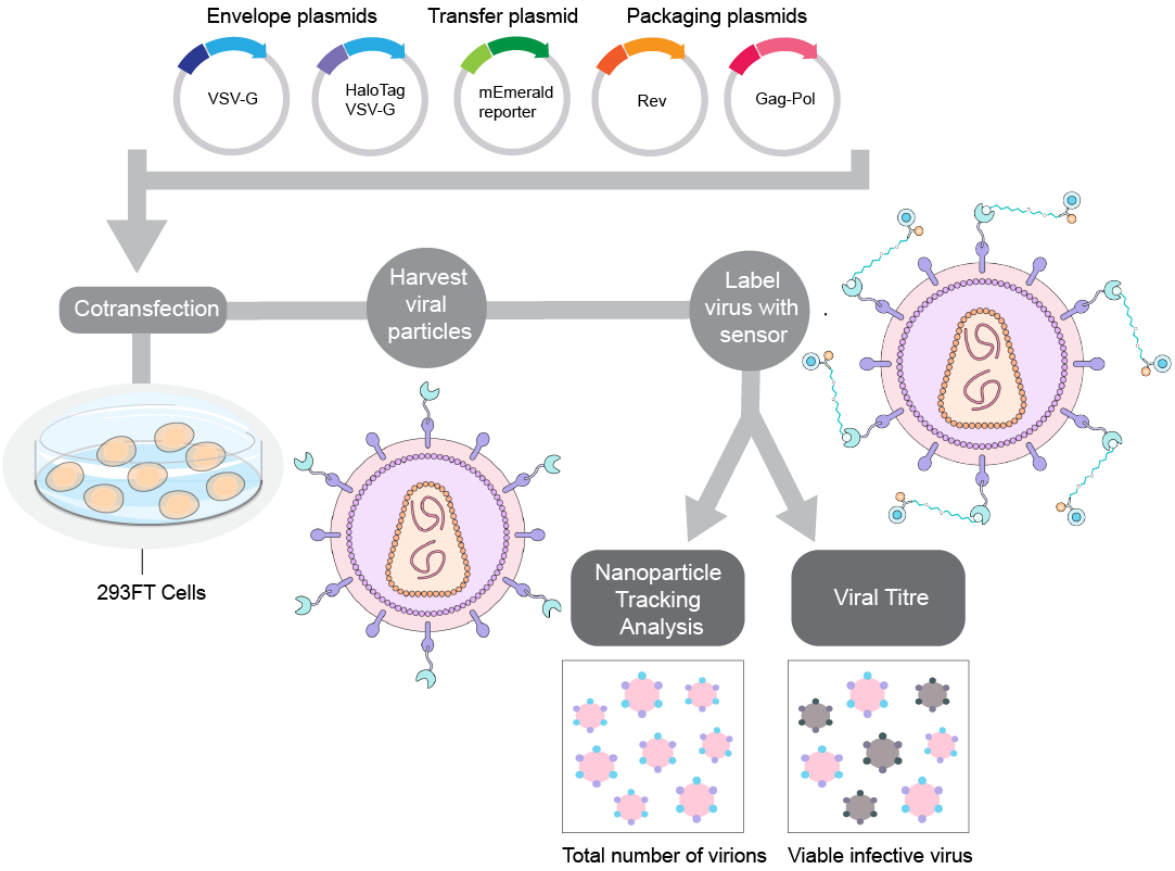

Figure 2-1 ***Visual representation of procedures for transient production of HaloTag-VSV-G tag pseudotyped lentivirus.*** *Processes include concentration and labelling steps followed by characterisation and quantification of viral particles using nanoparticle tracking analysis (NTA) and viral titering.*

2.2.1 Plasmid Design and Construction

The HaloTag-VSV-G Tag envelope plasmid was constructed by amplifying an envelope plasmid backbone (pCDH-EF1-MCS) through a PCR reaction and performing a Gibson HIFI DNA assembly reaction with the appropriate fragments. An mEmerald reporter gene transfer plasmid was also constructed through restriction digestion using EcoRI and NotI for both transfer plasmid backbone and a plasmid encoding mEmerald. All plasmids had been assessed for purity using gel electrophoresis and cleaned up using a PCR clean up kit before assembly.

2.2.2 Generation of lentivirus with 293FT cells

Lentiviral particles were produced by co-transfection of 293FT cells using Lipofectamine 3000 and P3000 enhancer reagent. 293FT cells were transfected with the transfer and envelope lentiviral plasmids along with Gag-Pol and Rev packaging plasmids in the following ratio (per 150 mm cell culture dish): 11 µg mEmerald-

expressing lentivirus vector, 5 µg gag/pol plasmid, 5 µg rev plasmid, and 2.75 µg of mixed ratios of VSV-G and HaloTag-VSV-G Tag plasmid depending on the ratio of HaloTag expression required. The two envelope plasmids were combined in a separate tube before adding the rest of the plasmids to ensure that all 5 plasmids would be taken up and expressed equally. After 24 h the transfection medium was changed, and the recombinant lentiviruses were harvested 48 h later.

2.2.3 Concentrating and labelling of generated lentiviruses

The virus particles containing supernatant were collected and filtered through 0.45 µM PVDF membrane filters. Then, the supernatant was centrifuged at 2000 rpm for 10 minutes at 25^{o}C and concentrated using Amicon purification system with 100kDa MWCO.

Viruses labelled via conventional click chemistry was performed with a molar equivalent excess of 2 mg mL^{-1} Sulfo-Cyanine 5 N-hydroxysuccinimide ester with an estimated concentration of virus particles based on NanoSight analysis. The mixture was performed in MilliQ water and kept at 4^{o}C overnight, followed by purification using a Zeba desalting column with a 7k molecular weight cut off.

The labelled viruses that expressed HaloTag fusion protein were instead labelled using HaloTag ligand succinimidyl ester (O4) building block conjugated to an amine group bearing the internalisation sensor. The harvested lentiviruses were then labelled with 1 µM concentration of internalisation sensor (Halo-sCy5-TCO) at 37^{o}C for 30 minutes and free sensor was removed using the same Amicon purification system with 100kDa MWCO.

All concentrated and labelled lentivirus was then aliquoted and stored at -80^{o}C until needed.

2.2.4 Validation through SDS-PAGE

Samples of labelled and unlabelled lentivirus were treated with 2-mercaptoethanol (βME) and loading dye (50 mM Tris-HCl [pH 6.8], 1% SDS, 8 mM EDTA, 0.01% bromophenol blue) and heated for 10 min at 95°C to achieve complete protein unfolding. The proteins were then separated by SDS-PAGE with the discontinuous system and 1.0 mm hand-cast 12.5% polyacrylamide gels using casting plates (Mini-PROTEAN Tetra; Bio-Rad, USA). PageRuler Plus prestained protein ladder (Range – 10 to 250 kDa; ThermoFisher Scientific, USA) were run in adjacent lanes. Gels were

analysed using fluorescent imaging (Amersham Typhoon FLA; GE Life Sciences, USA) with Cy2 and Cy5 channels acquired, and the data files were merged using ImageJ (2019).

2.3 Characterisation of Lentivirus

2.3.1 Viral Titre and Multiplicity of Infection Calculation

mEmerald titres were determined using 293 cells transfected with serial dilutions of labelled lentiviruses in the presence of polybrene at 8 μg/mL for 24 hours. Cells were then analysed for fluorescence with S1000EX flow cytometer (Stratedigm, USA) with the 488 nm blue and 642 red laser channels collected. mEmerald-positive cells were selected and calculated as transducing units (TU)/mL.

Multiplicity of infection (MOI) of lentiviruses were determined as the ratio of active viral units as indicated by the viral titre in TU/mL to the number of cells seeded on day 0 of experiments. An example of a calculated MOI of 5 would follow as such:

$$Total\ TU\ needed = (total\ number\ of\ cells\ seeded\ per\ well) \times\ (desired\ MOI\ of\ 5)$$

$$Total\ mL\ of\ lentiviruses\ to\ add\ per\ well = \frac{(Total\ TU\ needed)}{(\frac{TU}{mL}\ calculated\ from\ viral\ titre)}$$

Equation 1

2.3.2 Particle Sizing and Concentration Measurement

Nanoparticle tracking analysis (NTA) was also used for the counting and sizing of the labelled lentiviruses. Samples of lentiviruses were fixed with paraformaldehyde (PFA) and diluted between 1:100 to 1:250 to achieve an acceptable level of particles with the videos analysed using NTA 3.4 software and

calculated as total particles/mL.

2.3.2 Degree of Labelling Studies

AbC Total Antibody Compensation Bead Kit (Thermo Fisher Scientific, Cat# A10497) was used for estimating fluorescent signal from labelled lentivirus. Compensation beads were first incubated with anti-VSVG mouse antibody (Sigma-Aldrich, Cat# SAB4200695) at a 1:100 dilution at room temperature in the dark and washed with PBS as per manufacturer's protocol. The beads were then resuspended at an appropriate volume and calculated volumes of labelled lentiviruses were added and

left to incubate for 1h at room temperature on a ThermoMixer (Eppendorf, Germany) shaking at 500 rpm. Samples were then fixed with equal volumes of 4% paraformaldehyde prior to analysing using flow cytometry.

2.4 Internalisation Time Course Studies with Lentivirus

2.4.1 Quenching Efficiency and Internalisation

To calculate internalisation and quenching efficiency, the average mean fluorescence intensity (MFI) of the background (PBS for solution phase, control cells or negative control compensation beads for flow cytometry experiments) was subtracted from each sample. Quenching efficiency was calculated as a percentage from the following equation using the MFI (80):

$$\eta_Q = \left[1 - \left(\frac{Q_0}{N_0}\right)\right] \times 100$$

Equation 2

where η_Q = quenching efficiency, N_0 = MFI of the unquenched sample, and Q_0 = MFI of the unquenched sample.

Quenching efficiency was calculated using the same assay to quantify degree of labelling, where labelled anti-VSVG compensation beads were incubated with labelled lentiviruses for 1 h at room temperature on a ThermoMixer, shaking at 500 rpm before being split into quenched and unquenched groups after where the quenched groups were added an 5x excess molar equivalent of quencher QSY-Tet. The average quenching efficiency could then be used to compensate for incomplete surface quenching.

The percentage of material internalised, compensating for incomplete surface quenching, was calculated from the following equation (80):

$$I_f = \left[1 - \frac{N_1 - Q_1}{N_1 - \frac{N_1 Q_0}{N_0}}\right] \times 100$$

Equation 3

where I_f = fraction internalised, N_1 = MFI of the unquenched sample at 37 ^oC, Q_1 = MFI of the quenched sample at 37 ^oC.

2.4.2 Experimental Design and Flowchart

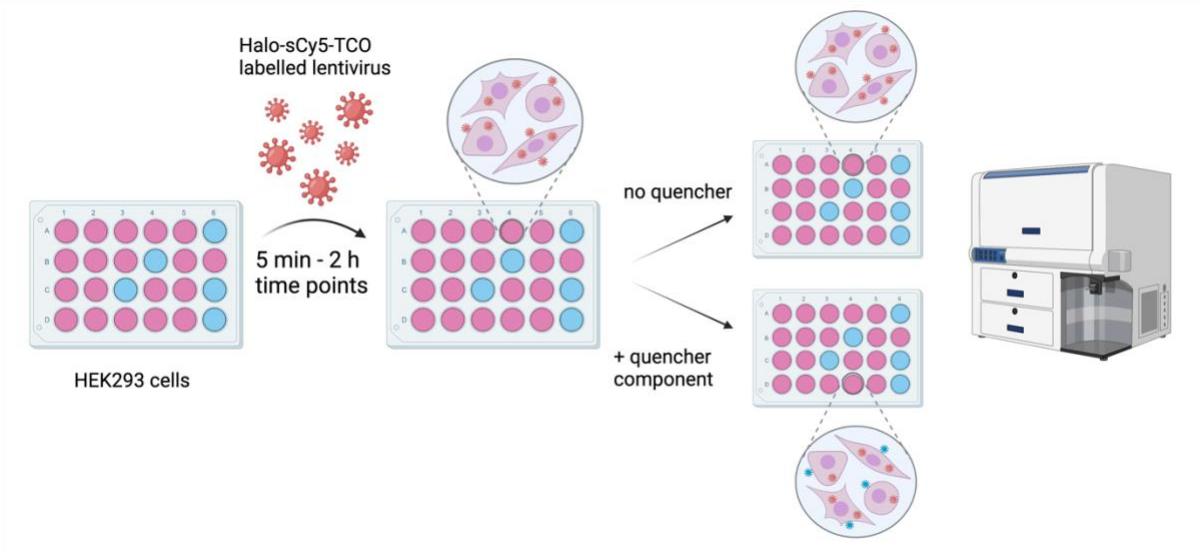

Figure 2-2 ***Visual representation of labelled Halo-sCy5-TCO internalisation sensor lentiviruses binding and internalised in HEK293 cells****. Multiple time points for incubation were performed, beginning from 5 minutes to 2 hours. Cells were then detached and split into groups with or without the addition of the quencher component before analysis by flow cytometry. Figure designed in Biorender.com*

HEK293 cells were seeded at 1 × 10^5 cells in 500 μL DMEM supplemented with 10% FBS per well in 24-well plates 1 day prior to the experiment (day 0) and were maintained at 37 ^oC in the incubator. A calculated MOI of 5 of labelled lentiviruses with Halo-sCy5-TCO was added per well at 5 min, 15 min, 30 min, 1h and 2h. The cells were then put on ice and washed twice in cold PBS before being detached with 100 μL TrypLE for 2 minutes. 100 μL of DMEM media was added to each sample and the entire contents were transferred to a 96 well V bottom plate. The cells were spun at 400 g for 5 minutes and resuspended in 50 μL PBS with or without 1 μM sQSY-Tet before analysis by flow cytometry. A simplified flowchart of the entire assay can be observed in Figure 2-2.

Chapter 3. Generation and Validation of Sensor Attached Lentivirus

Abstract

Lentiviruses are commonly used for basic biological research and have even emerged as a promising vector for gene delivery. It is important to further elucidate and determine viral uptake and internalisation kinetics of viruses to maximise therapeutic action in viral gene delivery. Surface modification of lentiviruses using conventional click chemistry has presented as inefficient as well as major loss in viral infectivity. Here we introduce the genetic incorporation of fusion proteins, HaloTag and the HaloTag ligand as an adaptor system to attach an internalisation sensor with minimal perturbation on virus physiology and demonstrating great flexibility. Not only does it allow for specific targeting on viral surface but can be more broadly useful with applications such as vector purification and immunomodulation.

3.1 Conventional Click Chemistry Attachment of Direct Sensor

Viruses commonly have densely packed surfaces, and there can be limitations on the location of the sensor conjugation as to not inhibit functionality or even assembly of the virus. Hence, particular care needs to be taken in choosing the most appropriate labelling approach as well as to ensure that the efficiency of the direct internalisation sensor is not compromised.

The most straightforward approach among the various techniques discussed for viral surface engineering would be the use of direct covalent modification involving traditional click chemistry. N-hydroxysuccinimide (NHS) and other activated esters are often used as coupling agents to covalently tether antibodies, enzymes, peptides, and other materials such as bioanalytical sensors on the surfaces via amide linkages (82). This reaction presents as convenient and straightforward as only a one-step aminolysis is required in a buffered aqueous and fairly neutral solution near physiological pH (pH 6 to pH 9) (83).

Vesicular stomatitis virus glycoprotein (VSV-G) is the most commonly used glycoprotein for pseudotyping lentiviruses due to its broad tropism, and ability to enable high-titre vector preparation (84). As a result, VSV-G pseudotyped lentiviruses were chosen as a platform to test NHS-mediated surface labelling. Wild type VSV-G

pseudotyped lentiviruses were transfected using HEK293FT cells and labelled with NHS-sulfo-Cy5 as a preliminary experiment to observe initial labelling efficiency and any potential effects on viral infectivity. Methods for generating lentiviruses and NHS labelling are as described in 2.2.3 Concentrating and labelling of generated lentiviruses. HEK293 cells were transduced with an MOI of 5 with the labelled lentiviruses for 24 hours before acquisition using flow cytometry as seen with Figure 3-1Figure 3-1 below.

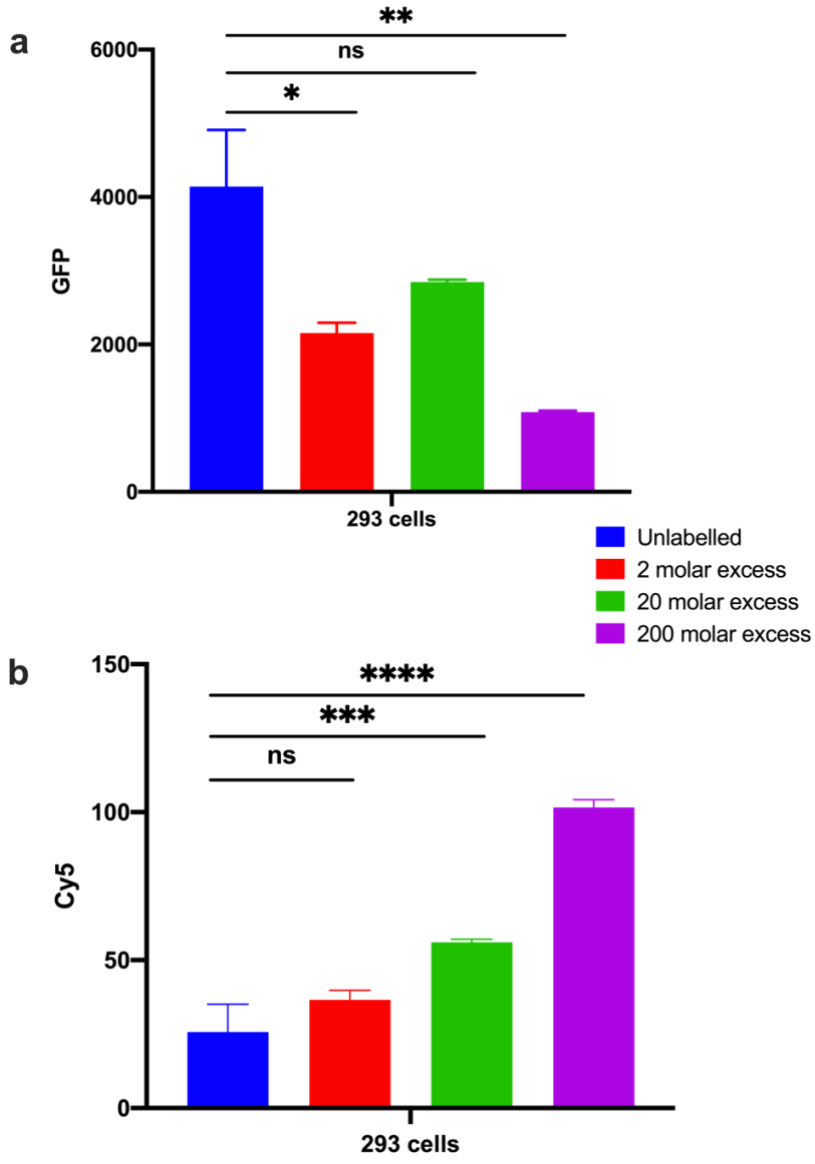

*Figure 3-1 Viral infectivity of NHS-sulfo-Cy5 labelled lentiviruses observed in HEK293 cells using mEmerald GFP expression in the GFP channel and labelling efficiency observed as Cy5 signal. (a) Mean fluorescence intensity in GFP channel of transduced HEK293 cell. (b) Mean fluorescence intensity in Cy5 channel. Groups observed were unlabelled (negative control) lentiviruses and lentiviruses labelled with 2, 20, and 200 molar excess of NHS-sulfo-Cy5 respectively. All groups were done in triplicates (n=3) ± standard deviation (SD). One-way ANOVA (GraphPad Prism) was used for the statistical significance analysis (where ns denotes $p > 0.05$, * $p \leq 0.05$, ** $p \leq 0.01$, *** $p \leq 0.001$ and **** $p \leq 0.0001$).*

NHS ester-mediated reaction involves the amine-reactive group with the primary amines presented on the viral surface, therefore it would be hard to calculate exactly the extent of labelling and whether the incorporation plateaus at a certain concentration. The amount of NHS-sulfo-Cy5 used for labelling was determined based on the number of total viral particles and the excess determined as molarity of Cy5 dye: molarity of viral surface protein. Lentiviral vectors contain 7-10 copies of the viral envelope surface glycoprotein *Env* and ≈ 2400 copies of the main structural protein *Gag* during its assembly from an immature viral particles (85). Each of these pseudotyped lentivirus particle would also be encapsulated with approximately 216 copies of VSV-G glycoproteins (86). This would translate as approximately an excess of 2 molar ratio based on the estimated viral proteins on the viral surface available for conjugation.

The highest Cy5 signal detected was with the lentiviruses labelled with 200 molar excess of NHS-sulfo-Cy5 with an average Cy5 signal of 101.6 ± 2.57, which was significantly different to the unlabelled group with an average signal of 25.73 ± 9.40. Comparatively, cells that were transduced with the unlabelled lentiviruses had the greatest expression of mEmerald GFP with average fluorescence signal of 4142 ± 1330 while cells that were transduced with lentiviruses labelled with the highest molar excess had an average signal of 1083 ± 33.5. This would demonstrate that the greater the excess of NHS used for labelling, the more compromised lentiviral infectivity, and the less expression of mEmerald GFP in cells, indicating that NHS mediated surface labelling are more applicable for more robust proteins and antibodies but may not be useful in preserving the stability and functionality of lentiviral surface proteins.

Moreover, there were concerns with the overall labelling efficiency of VSV-G glycoprotein species due to the nature of non-specific binding using NHS. This may result in varying densities of dye per viral particles across the viral population as the cross-linking is a random polymerisation process, which might even interfere with other viral protein stability (87). High ratios of NHS used can also increase non-specific background and loss of antibody binding affinity (88), as observed with antibody labelling of sulfo-Cy5 and the direct internalisation sensor, which also required protocol optimisation with a reduction in NHS labelling to minimize the amount of protein cross-linking that occurred, demonstrating the limitations of this method (80).

3.2 HaloTag Expression on Lentiviral Envelope Plasmid for Sensor Conjugation

While NHS labelling approach provided some justification for use with a detectable Cy5 signal, it presented inefficient, nonspecific binding and greatly affected viral infectivity, suggesting that a more succinct approach is required. Another approach was explored with using an adaptor system via genetic modification to ensure the most controlled way for bioconjugation.

Furthermore, this technique has also been previously described by Liu S. et al and Wang H. et al, where both papers described the expression of HaloTag at the C-terminus of HIV-1 Env. Although similar reduction in fusion efficiency was observed in all the HaloTag-attached envelope proteins, both papers observed that the fusogenicity of Env was preserved and HIV-1 viruses still retained membrane fusion activity (89, 90).

This use of self-labelling or enzymatic ligation, namely HaloTag ligand and HaloTag fusion protein is a commonly used approach for coupling biomaterials (91). The HaloTag is a 33kDa protein designed to covalently bind to its ligands while the HaloTag protein tags are modified haloalkane dehalogenase that are designed to covalently bind to synthetic ligands (92). The HaloTag ligands consist of a chloroalkane linker that can be attached to various useful molecules, such as fluorescent dyes and in this case, the internalisation sensor. The chloroalkane linker covalently binds to the active site of the HaloTag, displacing the terminal chlorine, generating a stable covalent bond between the ligand and the potential sensor (Figure 3-2) (93).

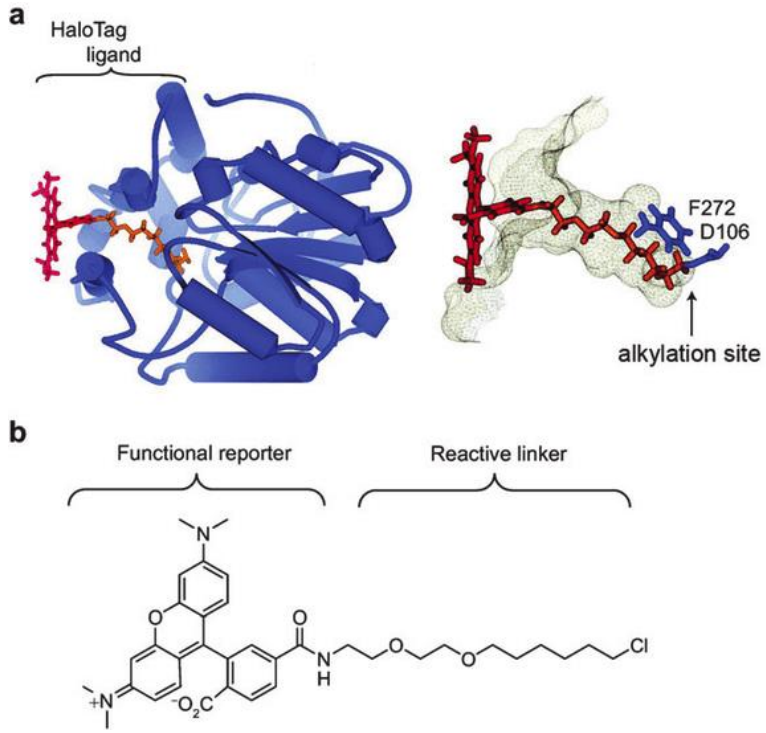

Figure 3-2 ***Rapid covalent attachment of HaloTag ligand with HaloTag protein through alkylation site. (a)*** *The HaloTag ligand (red/orange) fits in a binding pocket of the HaloTag protein.* ***(b)*** *The ligand has a fluorescent part and a reactive ligand with a terminal chloride (94). The binding of the HaloTag protein with a HaloTag ligand is rapid and irreversible, remaining relatively stable under a variety of conditions.*

The HaloTag-VSVG tag pseudotyped lentivirus would allow for an improved tolerance of structural alterations and minimal invasion since viral structural proteins are crucial in the assembly of stable multimeric structures (95). This domain represents a holistic and facile way to conjugate and label live viruses with other molecule sensors, allowing greater flexibility in comparing quantification methods for uptake and internalisation of different viruses and ensuring that viral function and infectivity is uncompromised.

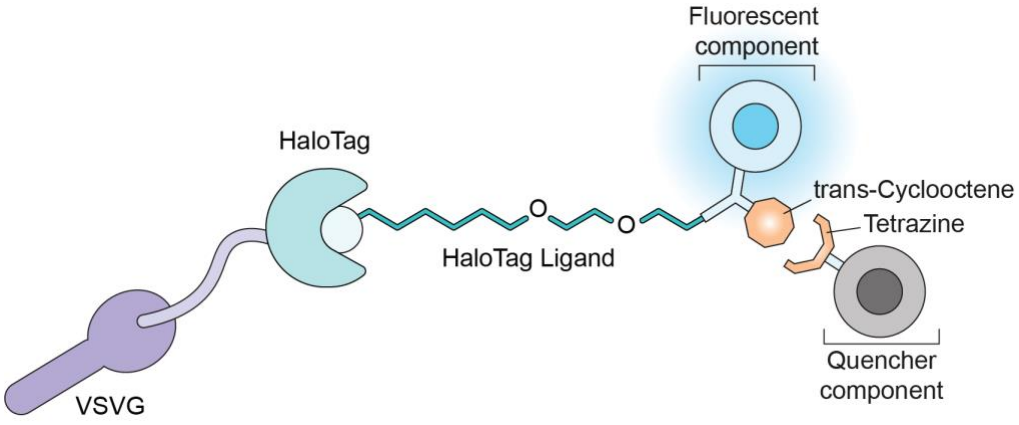

Figure 3-3 ***Labelling of VSVG protein through expression of HaloTag fusion protein.*** *Schematic representation of the click internalisation sensor developed by Selby et al. The fluorescent component (sCy5-transcyclooctene [TCO]) of the sensor can be attached to VSVG protein that has HaloTag expressed on the surface. Signal from click internalisation sensor can be rapidly quenched with the addition of a compatible click group with a quencher component (sQSY-Tetrazine [Tet]) (80).*

To begin the generation of modified pseudotyped lentiviruses, we first aim to establish a succinct method for the lentiviral production that involves the HaloTag ligand labelling. Extensive development and optimisation of lentiviral production techniques have already been demonstrated in research and in most cases, lentiviruses are traditionally produced by transient transfection of 293 or 293T cells (96-98). Third generation lentiviral vector systems were developed to increase the use and safety of lentiviruses in consideration of the pathogenicity of HIV-1 in humans. It is a four-plasmid system, consisting of two packaging plasmids, one envelope plasmid, and one gene transfer plasmid. Packaging plasmids include *gag-pol*, which includes for the structural proteins and viral enzymes, and *rev* encodes for a post-transcriptional regulator (99).

While lentiviral vectors can be pseudotyped with different heterologous envelope glycoproteins (100), most vector preparations including this project uses the glycoproteins of the vesicular stomatitis virus (VSV-G) envelope as it broadens the host range and stabilises the viral particle. The transfer plasmid is the only genetic material transferred to the target cells and acts as an indicator of transduction efficiency, providing a way to quantify viral titres. Green fluorescent proteins are most commonly used as reporter genes and in this project, an mEmerald variant fluorescent protein was chosen for this project as it has improved photostability along with increased brightness than other green fluorescent proteins (101).

Initial development involves the construction of viable envelope and transfer plasmids used in the assembly of these lentiviruses since the HaloTag would be expressed on the surface of the viral membrane, followed by general transfection protocol with HEK293FT cells then harvesting and concentrating the lentiviral samples.

To address this, we first looked at the design of transfer plasmid containing an mEmerald reporter gene and an envelope plasmid with the VSVG tag protein to include the appropriate sequence for HaloTag fusion protein.

3.2.1 Generation of mEmerald GFP Transfer Plasmid

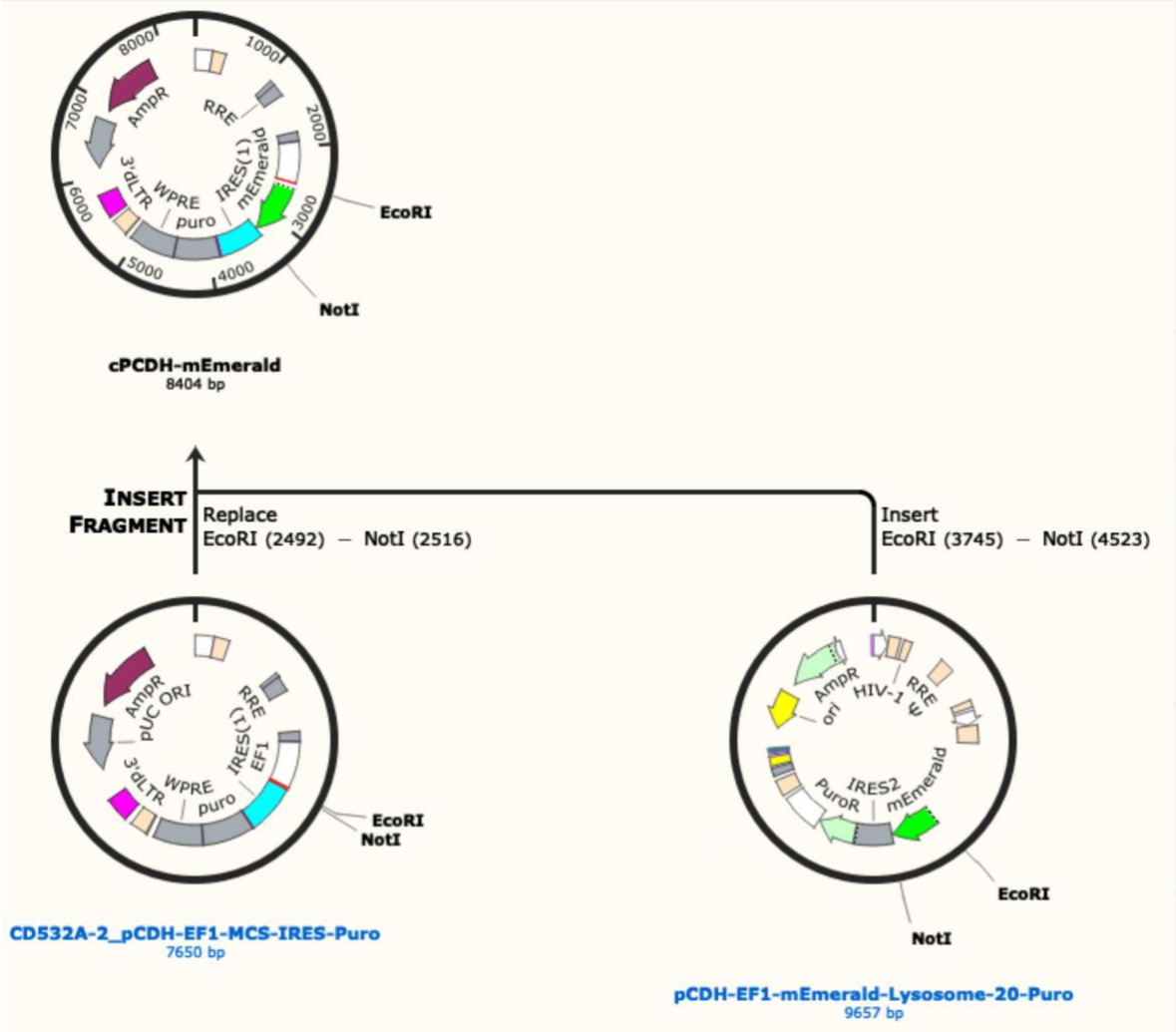

Figure 3-4 ***Plasmid maps for empty backbone plasmid (bottom left) and mEmerald sequence (bottom right)****. Generation of mEmerald lentiviral transfer plasmid (top left) after digestion and re-insertion using EcoRI and NotI. Plasmid maps were generated using SnapGene software.*

The transfer plasmid was generated with an enzyme digestion of the empty backbone (pCDF-EF1-MCS-IRES-Puro) and the plasmid containing the mEmerald sequence (pCDH-EF1-mEmerald-Lysosome-Puro) using enzymes EcoRI and NotI as shown in Figure 3-4. Following the digestion, the next step was to ligate the mEmerald sequences with the appropriate transfer plasmid backbone and subsequent bacterial transformation and colony selection for plasmid preparation. A restriction digest with EcoRI and NotI for the plasmid was done to verify the mEmerald sequence with the colonies selected from the transformation shown in Figure 3-5. Since the mEmerald sequence was calculated to be 720 bp in size, the faint band from colony 1 lane is corresponds to the approximate range of 700 to 750 bp and the plasmid sequence validated and prepared for large scale plasmid preparation.

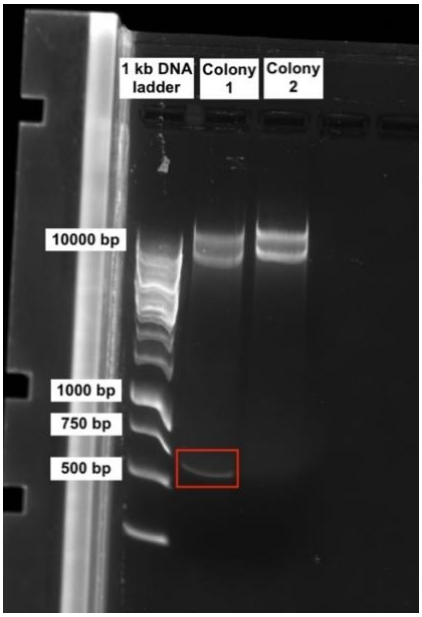

Figure 3-5 ***Gel electrophoresis image of plasmid DNA collected****. DNA sequences were purified from colony 1 and 2 after bacterial transformation of ligated mEmerald sequence and transfer backbone. Restriction digest with the enzymes EcoRI and NotI were then performed. The faint band highlighted in red from colony 1 lane corresponds to the appropriate mEmerald sequence.*

3.2.2 Generation of HaloTag VSV-G Tag Envelope Plasmid

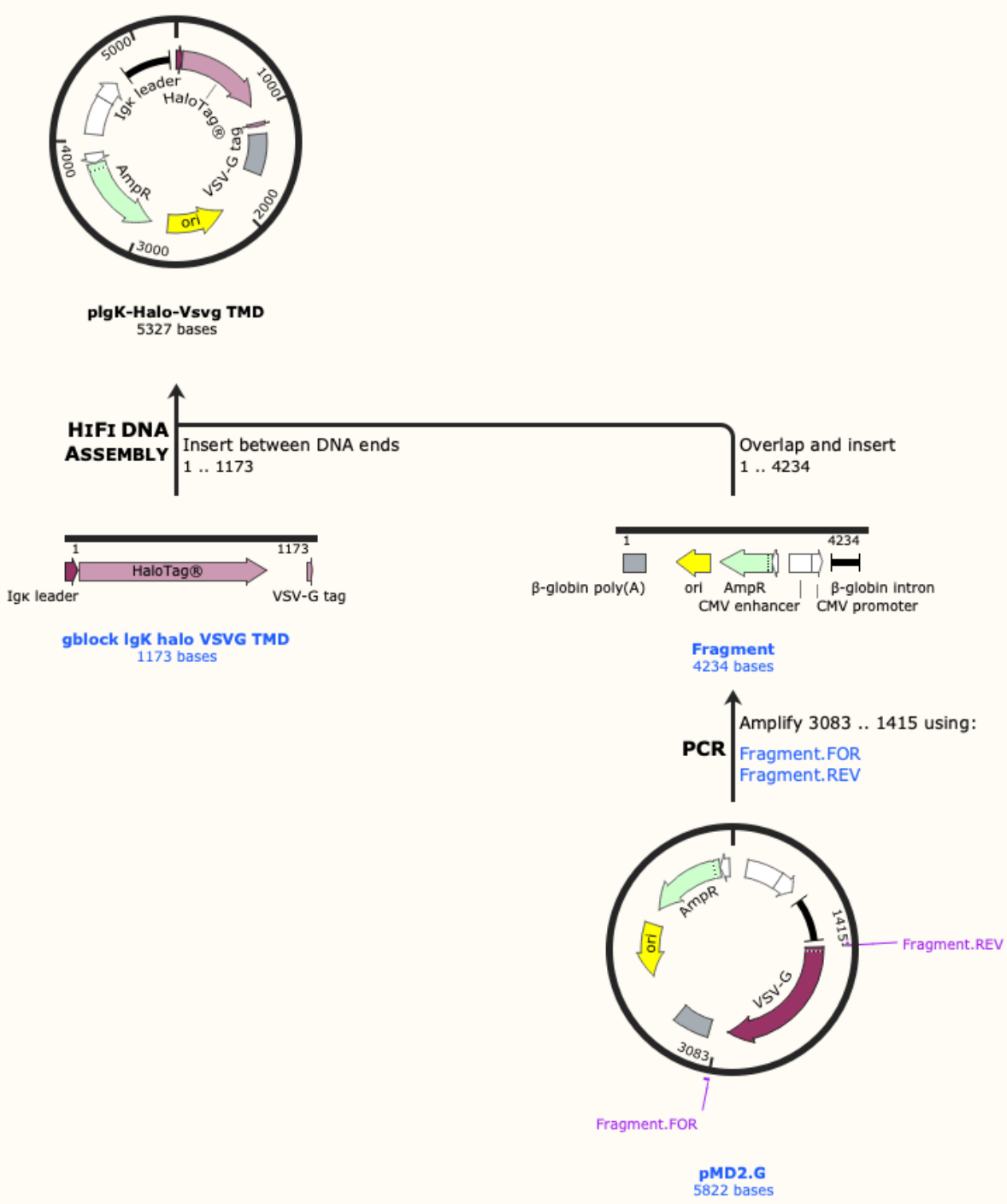

Figure 3-6 ***Generation of plasmid vector of the HaloTag VSV-G envelope sequence (top left).*** *Initial amplification of an empty pMD2.G VSV-G envelope plasmid (bottom right) followed by a Gibson assembly with gBlock containing sequence of HaloTag and VSV-G Tag. Plasmid maps were generated using SnapGene software.*

The VSV-G envelope vector expressing the HaloTag fusion protein also had to be designed and constructed as seen in Figure 3-6. pCMV-VSV-G was used as the empty backbone vector for the construction of the HaloTag-VSVG plasmid, beginning with a restriction digest using EcoRI enzyme and followed by a gel extraction and purification

of the vector backbone. A gBlock fragment that was initially contained HaloTag fusion protein followed by a VSV-G epitope tag was designed to be inserted into the backbone, but the fragment was mistakenly ordered without the overhang primers. Therefore, primers with the additional overlapping ends had to be ordered and used for PCR amplification of the gBlock fragment before the Gibson assembly could be performed. Subsequently, the Gibson assembly product was then used for bacterial transformation and the colonies selected for miniprep and verification. Similarly, the purified plasmids were digested with EcoRI to confirm the HaloTag-VSVG tag.

Both mEmerald and HaloTag-VSVG tag plasmids were sent for Sanger sequencing for confirmation before the preliminary lentiviral production began.

3.2.3 Assembly and Verification of Preliminary Lentiviral Production

After optimisation of the HaloTag-VSVG envelope and mEmerald transfer plasmids, HEK293FT cells were seeded in 1 mL culture volume for virus production. The cells were then transfected the next day with the appropriate ratio 6:4:1:1 of transfer: GagPol: Rev: envelope vectors respectively with lipofectamine 3000 with an OptiMEM media change 24 hours post transfection based on optimised protocols (102). Ratio of HaloTag expression could be controlled by assuming that adjusting the ratio and amount of different envelope plasmid added during transfection would result in a difference in the expression. For example, lentiviruses with 100% wild type VSVG that had no HaloTag expression were produced using only the wild type VSVG envelope plasmid while lentiviruses with 50% HaloTag-VSVG tag: 50% wild type VSVG would require an equal amount of both wild type VSVG and HaloTag-VSVG tag envelope plasmid.

In total, 4 different combinations of wild type VSVG to HaloTag-VSVG lentiviruses were made:

1. 100% wild type VSVG
2. 75% wild type VSVG: 25% HaloTag-VSVG tag
3. 50% wild type VSVG: 50% HaloTag-VSVG tag
4. 100% HaloTag-VSVG tag

All lentiviruses were then concentrated before labelling with an excess amount of commercial fluorescent Cy-5 HaloTag ligand to observe the initial conjugation. Identity

of the lentiviruses was confirmed using SDS-PAGE shown in Figure 3-7, with the viruses boiled at 92^{o}C and loaded with loading dye and run at 100 volts for 1 hour.

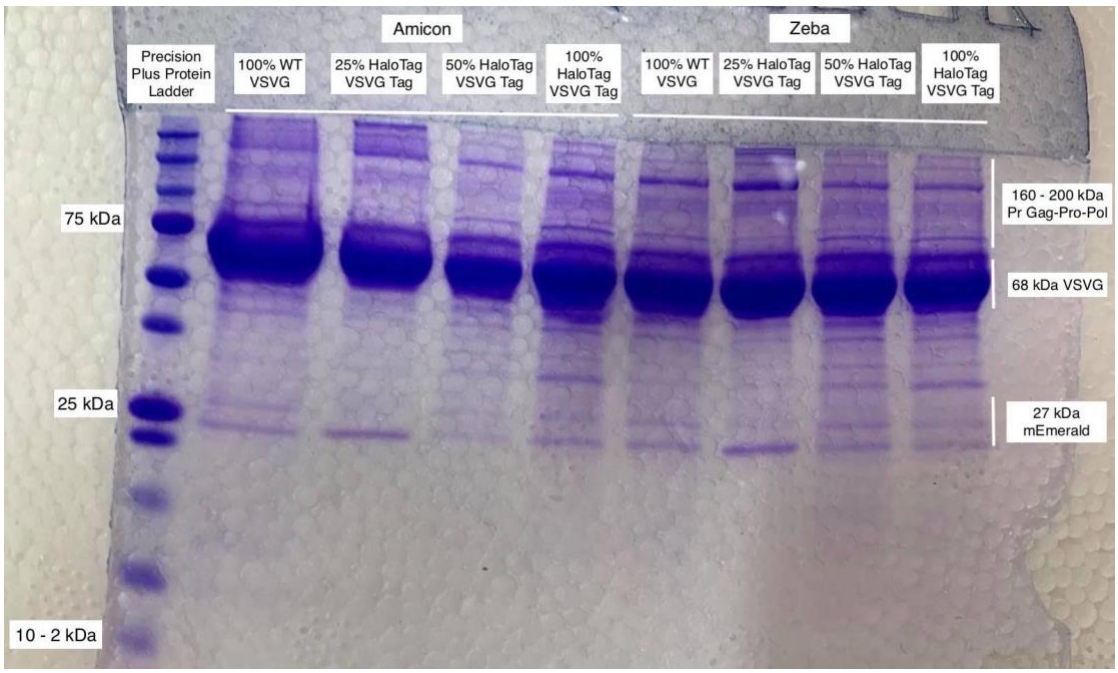

Figure 3-7 ***Verification of assembled HaloTag-VSVG tag envelope pseudotyped lentivirus.*** *Reducing SDS-PAGE of HaloTag conjugated VSVG lentivirus with varying ratios of transfer plasmids (wild type VSVG protein and HaloTag VSVG tag protein), displaying successful lentiviral transfection and production with the required transfer (mEmerald) and packaging plasmids (Rev, and Gag-Pol).*

Since a reducing gel was used, the viral proteins would be separated and therefore the VSVG protein and the mEmerald reporter protein could be easily distinguishable along with the other Rev, Gag-Pol packaging proteins. The HaloTag-VSVG tag is visible in Figure 3-7 at the 75 kDa band. Multicolour fluorescence typhoon imaging was also performed to observe the HaloTag ligand conjugated to the HaloTag protein on the VSVG-tag, as shown in Figure 3-8.

3.2.4 Labelling Method Optimisation Post Lentiviral Transfection

An extra band can be seen for lanes with lentivirus expressing HaloTag-VSVG, which suggests that the HaloTag protein may have been expressed separately from the glycoprotein or that the excess fluorescent protein may have associated with the wild type glycoproteins since a ratio of wild type VSVG to HaloTag-VSVG tag was used.

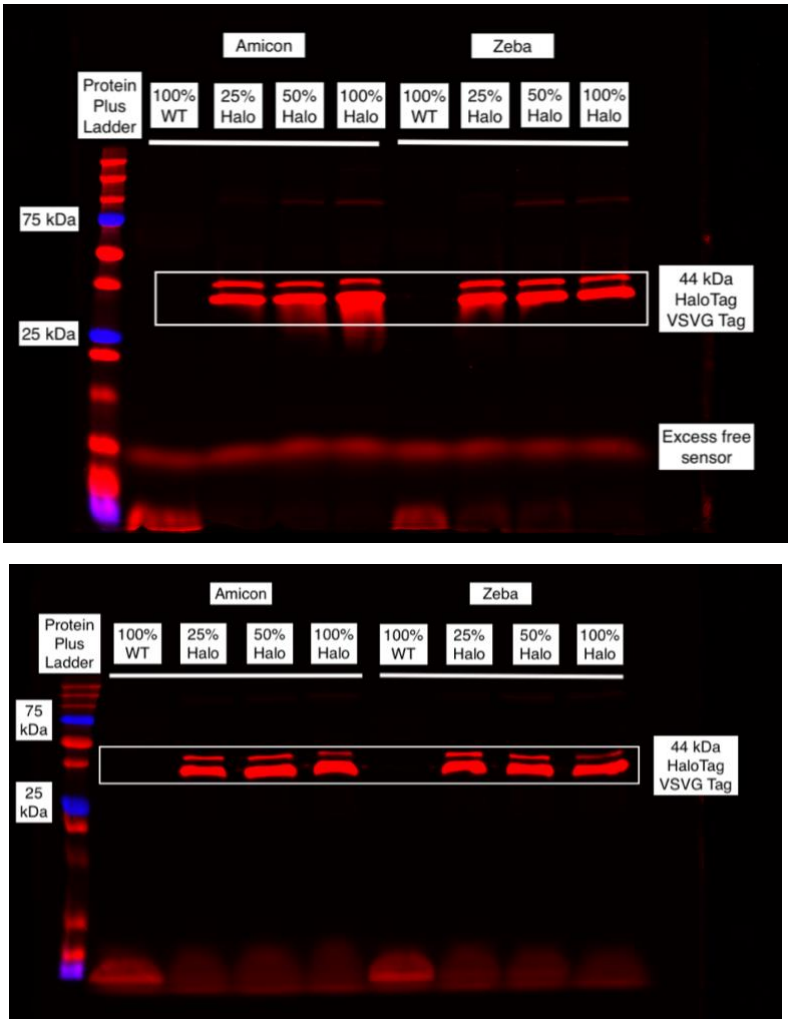

Figure 3-8 ***Additional wash step included removes excess free HaloTag-sCy5 substrate.*** *Representative typhoon imaging of denatured labelled lentivirus that were purified either using 100k Amicon concentrators or Zeba desalting columns (top) and denatured labelled lentivirus that had no purification step after labelling (bottom). All groups of lentiviruses were labelled with commercially available fluorescent HaloTag-Cy5 ligand. Both lanes on far-left presenting protein ladders with molecular weight range of 10 – 250 kDa.*

Preliminary data from the imaging revealed an area of concern – the excess labelling with the lentiviruses. One reason for the excess Cy5 signal detected among the groups of lentiviruses could be due to the lack in purification after labelling. In the current protocol, there was no wash step included after the Halo-sCy5-TCO sensor has been added to the lentivirus, suggesting that the increase in Cy5 signal could be due to the free sensor remaining in the sample. Therefore, a wash step to remove any free sensor was introduced into the protocol, and 100k Amicon concentrators and Zeba desalting columns were tested to determine the better recovery for labelled lentiviruses. Once this extra step has been established and included in the final protocol, it has significantly improved recovery of labelled lentiviruses while ensuring minimal background signal from excess dye or in future cases free excess internalisation sensor.

3.3 Optimisation HaloTag Expression on Lentiviral Surface Membrane

All 4 combinations of ratios of HaloTag VSV-G tag lentiviruses were made and the impact of the HaloTag incorporation infectivity as well as strength of signal from the internalization sensor was determined. Viruses were labelled with an excess concentration of HaloTag-sulfo Cy5-transcyclooctene (TCO) internalisation click sensor and purified using a 100 kDa Amicon filter as per protocol mentioned above.

Transduction assays examining expression of the GFP mEmerald transgene, shown as MFI values in the GFP channel, in HEK293T cells exhibited a reduction of functional titre (TU/mL) as the ratio of HaloTag VSVG tag expression, which was the amount of HaloTag VSVG tag envelope plasmid used during transfection, increased.

Interestingly, the Cy5 signal generated from the internalisation sensor readily increased as the ratio of HaloTag VSVG tag increased and plateaued at higher ratios. Two things should be highlighted based on this initial experiment. Firstly, the expression of HaloTag fusion protein on the VSVG tag allowed the conjugation of the internalisation sensor as evidenced by the increase in Cy5 signal. But also, the infectivity of HaloTag VSVG tag lentiviruses decreases as the ratio of HaloTag VSVG tag on the viral surface increases, suggesting that while the VSVG epitope tag's ability to attach and fuse with the host cellular membrane to enter the cell, the HaloTag fusion protein is potentially limiting the viral-induced pH-dependent endosomal membrane fusion. It is also observed that the ability of VSVG to enter a cell does not guarantee successful virus application. This brings another suggestion that the HaloTag VSVG envelope plasmid might impact on the successful assembling and packaging of the virus and subsequent viral gene transcription and genome replication could also be inhibited.

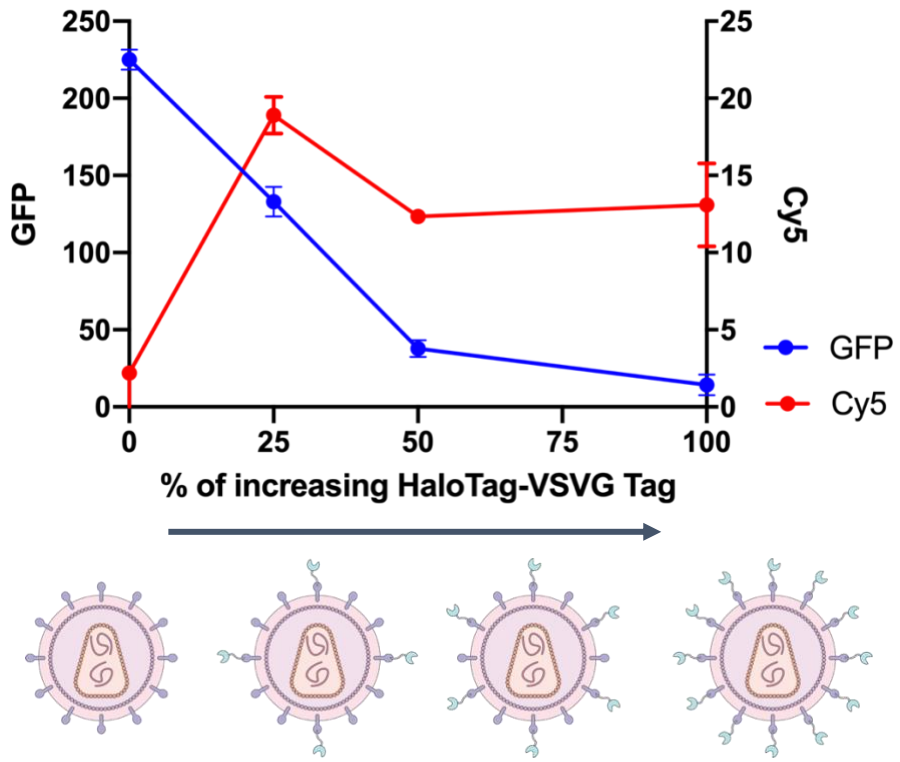

Figure 3-9 ***Increasing HaloTag-VSVG tag expression affects viral infectivity.*** *Varying ratios of HaloTag-VSVG tag to VSVG wild type were selected for lentiviral construction, starting from 100% wild type VSVG, 100% HaloTag-VSVG tag, 75% wild type: 25% HaloTag, 50% wild type: 50% HaloTag respectively. GFP channels represent lentiviral infectivity with mEmerald expression while Cy5 channels represent signal of fluorescent click sensor conjugated to lentiviruses. Experiments were performed in triplicates (n=3)*

Despite this, the results observed still shows promising potential in the use of HaloTag expression as an adaptor system to conjugate the internalisation sensor as the ratio of HaloTag expression could be optimised to ensure that there are minimal effects on infectivity and can be closely monitored with the GFP mEmerald transgene expression, but also maintain a high level of labelling as observed with the Cy5 signal on the internalisation sensor. With these factors in mind, the optimal ratio of HaloTag VSVG tag expression on lentivirus was observed to be 25% HaloTag VSVG tag: 75% wild type VSVG. Unless explicitly stated, following chapters with the labelled lentivirus will be transfected with this ratio.

Following from this experiment, the next two chapters will be demonstrated with the optimised lentivirus for further characterisation and used to study the labelling and quenching efficiency of the internalisation sensor on lentiviruses and observe the internalisation kinetics of the lentiviruses in HEK293 cells.

Chapter Summary

Currently, there are still no standardised procedures for the labelling of live viruses and methods vary greatly between enveloped and non-enveloped viruses. Non-enveloped viruses such as adenoviruses are structurally more robust than enveloped viruses, which are surrounded by a lipid bilayer membrane that is obtained from the host cell membrane during the budding process. Since any membrane disruptions may also inadvertently affect viral infectivity and functionality, a more gentle and non-disruptive labelling strategy is required (103).

Covalent labelling using conventional NHS click chemistry has been commonly used for adenoviruses, however, this study has demonstrated the inefficient and non-specific labelling for enveloped lentiviruses with significant effects of viral health and activity. Most studies are also observe that this technique would be more suited for nonenveloped viruses, where the capsid is exposed to the outside as well as for studies that do not require specific and controlled labelling of the viruses (40).

In summary, this chapter demonstrates the utility of HaloTag fusion protein as an appropriate technique for lentiviral surface conjugation. HaloTag self-labelling systems have been used in numerous applications, and in this case, its use as an adaptor system provides a versatile and flexible way in conjugating biomolecule sensors to lentiviruses to observe viral internalisation without affecting infectivity. This method presents a highly robust and generalisable approach for labelling lentiviral surfaces.

Lentiviral vectors were chosen for expediency, but in principle this method will be accessible with any virus bearing other surface glycoproteins. Additionally, the controlled expression of the HaloTag protein on the surface presents an effective way for ensuring high specificity and regulation in the degree of labelling or conjugation on viral surfaces.

Chapter 4. Characterisation and Degree of Labelling Studies

Abstract

In previous chapters, we have established and optimised lentiviral transfection and labelling protocols to produce HaloTag expressed lentiviruses conjugated to Halo-sCy5-TCO internalisation sensor. Ratios of HaloTag expression were observed lentiviral infectivity and sensor activity and a chosen ratio of 25% HaloTag-VSVG Tag expression based on plasmid DNA concentration was determined to be the most appropriate for further *in vitro* studies. Here, we continue to investigate and characterise lentiviruses including measurements of particle size, viral titres, and physical particle counts, all of which are basic evaluation of structural stability and infectivity. Determining viral titres as well as sensor activity studies were successfully performed with anti-VSVG antibody reacted compensation beads on flow cytometry while viral sizing and counting at the single particle level was completed by nanoparticle tracking analysis. These results demonstrate the utility of the internalisation sensor with lentiviruses without compromising infectivity and has significant potential to observe viral internalisation in cells.

4.1 Importance in Lentiviral Characterisation

The study of viral vectors in academic laboratories and in industry for both research and clinical applications have been commonplace for decades. Lentiviral vectors have been approved as therapy for primary immunodeficiencies and cancers due to their ability to more efficiently transduce non- or slowly proliferating cells, such as CD34+ stem cells (99). Rigorous and extensive assessments are done on the lentiviruses to characterise and ensure that the batch-to-batch consistency and potency of the viruses are replicable.

Lentiviral vector screening includes multiple aspects such as vector functionality, encompassing quantification of vector RNA, protein and enzyme activity as well as determining functional titres and evaluating actual viral particle size and concentration. For example viral protein expression can be analysed by enzyme linked immunosorbent assay (ELISA), SDS-PAGE or any form of total protein quantification (104). Alternatively, quantifying viral titres can be done with assessing reverse transcriptase (RT) activity and the viral RNA content in supernatants, as well as the number of pro-viral DNA and the efficacy of transgene expression in transduced target

cells (105). Each provide their own set of benefits – assessing RNA contents has higher throughput and provides the most rapid turnaround while assessing vector expression in transduced cells have better estimation of functionality and potency. Evaluating physical viral particles is also essential in the characterisation of lentiviral vectors. Dynamic light scattering (DLS) and nanoparticle tracking analysis (NTA) are both complementary techniques to quantify physical particle counts and assess mean particle size, polydispersity and particle size distribution. This also provides a tool to determine if the viral batch is aggregating and determines overall stability of the sample (106).

The transfection protocol for HaloTag-VSVG Tag lentivirus has been established and the ratio of HaloTag expression on the envelope surface has been established in the previous chapter. Next, we aim to address the aims of thorough characterisation of labelled lentiviruses, beginning with sizing followed by determining both total viral particle titre and infectious virus particle titre given in transducing units (TU) per mL.

4.2 Characterising HaloTag-VSVG Tag Lentivirus

4.2.1 Particle Size of HaloTag-VSVG Tag Lentiviruses using NTA

Briefly, particle size of the labelled lentiviruses was determined using nanoparticle tracking analysis (NTA) as described in Chapter 2, Section 2.3.2 Particle Sizing and Concentration Measurement.

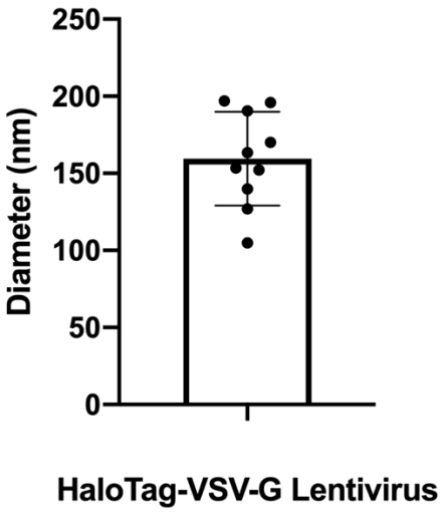

Figure 4-1 ***Average hydrodynamic radius of labelled HaloTag-VSVG Tag pseudotyped lentivirus.*** *Lentiviruses were fixed with 0.1% paraformaldehyde before acquisition with NanoSight nanoparticle tracking analysis (NTA) software 3.4 (Malvern). Each data point represents a diluted sample for a different batch of lentivirus transfected. Each data point was acquired 5 times for 60-seconds each time. 10 separate batches of lentiviruses were transfected in total whereby n=10 ± standard deviation (SD).*

The average diameter of virus was calculated to be 160 ± 10 nm as seen in Figure 4-1, similar to reports of unmodified virus particles (86), suggesting that the addition of the internalisation sensor did not significantly affect particle size. It was also noted that the lack of virion aggregates during analysis demonstrates that the purification process using Amicon filters post labelling did not impact on the recovery of the lentiviruses and suggested some level of heterogeneity and therefore increased stability of the sample.

4.2.2 Functional Viral Titre vs. Total Particle Concentration

Next, functional viral titre as well as total physical counts of viral particles were performed. Functional titres provide a more accurate method to quantify viruses as the concentration is based on the analysis of transgene expression of successfully infected cells.

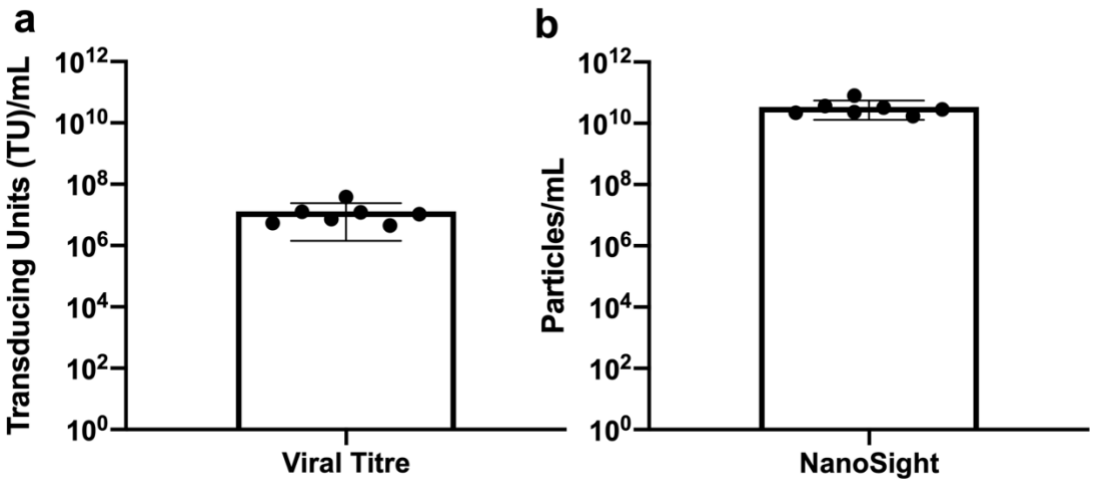

Figure 4-2 ***Viral titre and NanoSight concentrations for infective HaloTag-VSVG Tag lentivirus.*** *Viral titres are expressed in transducing units (TU) per mL (viral titre) while NanoSight concentrations in total physical particles in particles per mL (NanoSight). Each data point represents a different batch of lentivirus produced and a total of 7 replicates were performed (n=7) ± standard deviation (SD).*

The average NanoSight concentration as seen in Figure 4-2 was calculated to be 3.5 ± 0.8 × 10^{10} particles/mL while the mean functional viral titre was 1.30 ± 0.4 × 10^{7} TU/mL. Transducing units measures functional vector particles that results in the expression of a fluorescent reporter protein and depends on the titration conditions. For example, the total volume the cells are covered in, the incubation time and level of dilution can all affect titre estimation significantly. In addition, because this assay is replication dependent, it assumes that the level of expression of all the integrated vectors is above the detection threshold of the assay and may not distinguish cells

with multiple copies of the vector, often resulting in an underestimation of titre concentration. Viral titre may provide useful insight in viral assembly and packing, but also in viral uptake, endosomal escape, and localisation, which may be different for different cell types.

While a 3-fold difference between the two titre and particle concentrations are observed, these represent the different methods to roughly estimate the concentration of the sample, be it only infectious transducing units or total counts of physical particles would be beneficial in the characterisation of lentiviruses.

Additionally, the successful production of infectious viral particles can be disrupted or inhibited by almost any steps during replication and as seen with HIV viral production, there is often a high frequency of mutations introduced in the genome that can contribute to the production of defective or dead virus particles (107, 108). It is estimated that approximately 1% of virus particles in an HIV-1 infected individual that are actually infectious (109). Therefore, it is comparable that HaloTag expressing lentiviruses produced will inevitably contain several defects in the viral genome based on the inefficiency of the viral assembly process and not necessarily on the labelling process with the internalisation sensor.

4.3 Characterising Halo-sCy5-TCO Internalisation Sensor on Lentiviruses

Following the physical characterisation of lentiviruses, the labelling and quenching efficiency of the internalisation sensor was evaluated. The sensor was characterised with the use of flow cytometry compensation beads, commonly used for the setting of flow cytometry compensation, that had antibody conjugate capture capacity. In this case, anti-VSVG antibody was prebound with the compensation beads prior to reacting with the labelled lentiviruses. This provides an appropriate technique to discriminate viruses from the typically nonfluorescent background noise typically observed in flow cytometry.

4.3.1 Optimising Sensor Activity Assay with Compensation Beads

Incubation time for labelled lentiviruses with compensation beads was optimised within a linear range to ensure that compensation beads were completely saturated and consistent in between replicates. Results in Figure 4-3a suggested that 1 hour incubation provided adequate signal for detection and any more than 1 hour incubation resulted in significantly variable results. This could be a result of incomplete saturation

of the labelled lentiviruses on the compensation beads as the initial ratio selected to test out incubation times could be too low.

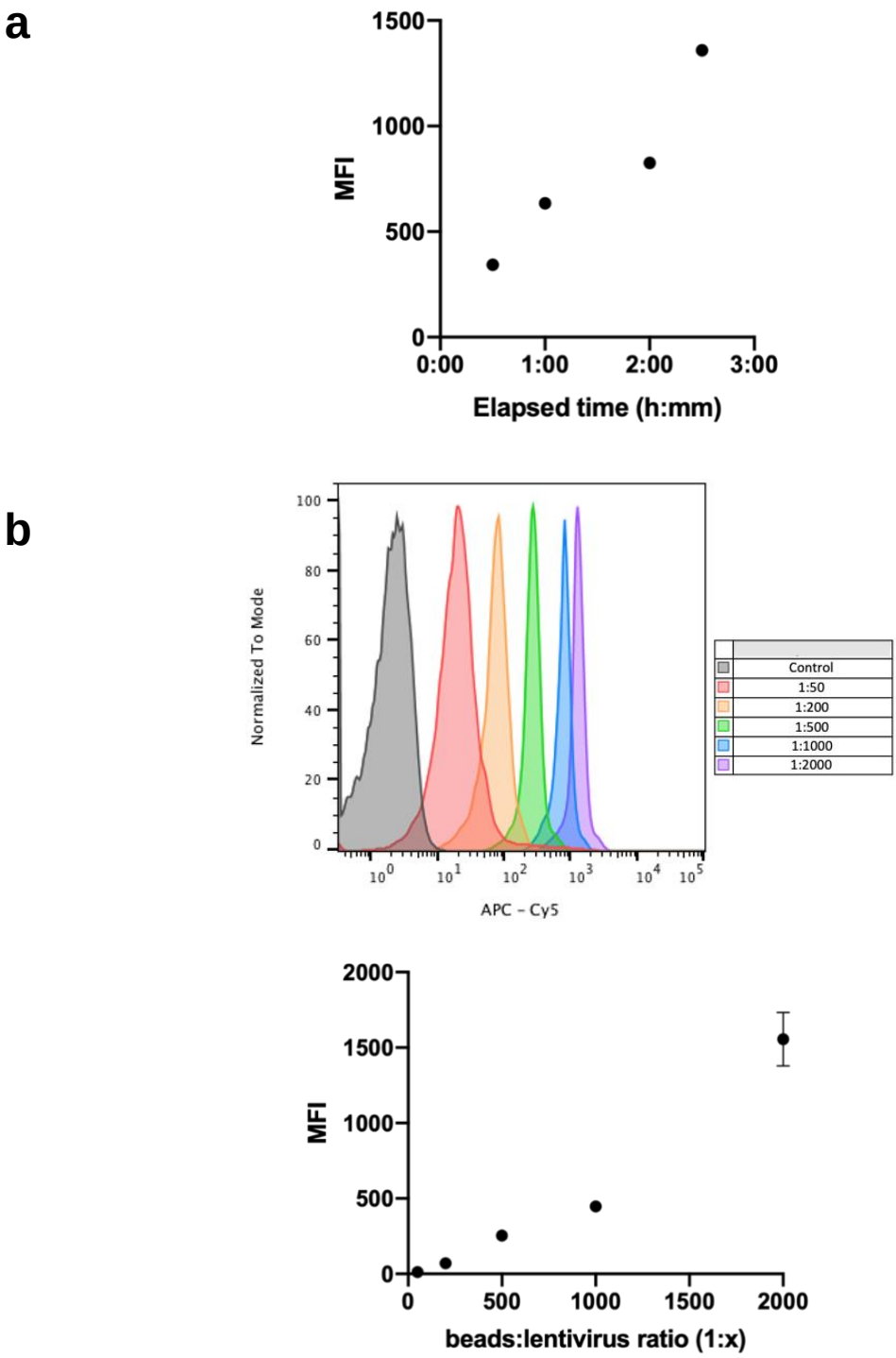

Figure 4-3 ***Optimising incubation times and ratios of labelled lentiviruses with compensation beads.*** *(a) Representative graph observing the increase in Cy5 signal of internalisation sensor with increasing incubation times followed by (b) Representative flow cytometric plot and graph of increasing ratios of lentiviruses on compensation beads to determine labelling efficiency of Halo-sCy5-TCO internalisation sensor. Each data point in both graphs were performed in duplicates and each assay was performed in triplicates (n=3) ± standard deviation (SD).*

Next with the optimised incubation time, 5 different various ratios of lentiviruses were added to compensation beads to determine the MFI of a single lentivirus based on a single compensation bead with both concentrations known. In Figure 4-3b, a linear trend can be observed between the data points, with an increase in lentiviruses to compensation beads results in an increase in MFI signal. Linear regression was calculated based on the trends of data points and the proposed equation to calculate MFI of a single virus labelled with an internalisation sensor based on a single bead was

$$y = 0.6992x$$

Equation 4

This would suggest that associating labelled lentiviruses with antibody capture beads, the fluorescence intensity of single virion particle can be determined. With this equation, it is suggested that one virion labelled with Halo-sCy5-TCO internalisation sensor would result in an MFI of 0.6992. This demonstrates high sensitivity of the molecular sensors with flow cytometry compared to other fluorescence assays.

4.3.2 Quenching Efficiency of Internalisation Sensor

The efficiency of the QSY-Tet quencher component was compared with the use of compensation beads and *in vitro* using HEK293 cells as seen in Figure 4-4. Experiments with both groups were performed at 4°C to observe activity of the sensor when cellular internalisation is halted. The quenching efficiency of QSY-Tet with compensation beads was observed to be ~71%, establishing that the quencher could switch off signal from the fluorescent component in solution.

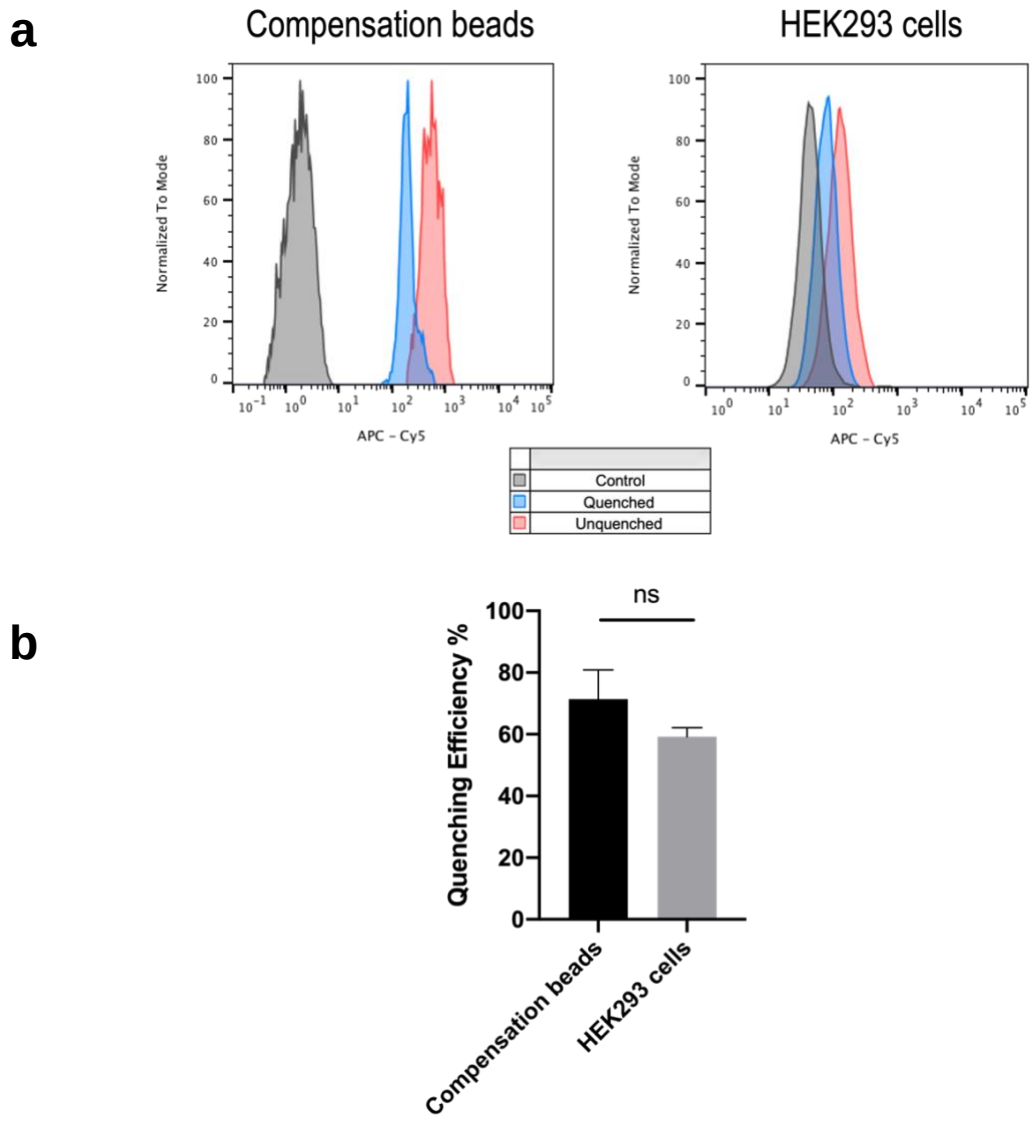

Figure 4-4 ***Quenching efficiency of internalisation sensor is comparable when used with compensation beads or in vitro in HEK293 cells.*** *(a) Representative flow cytometry plots of quencher activity in compensation beads and HEK293 cells including an unlabelled control group shown in grey with no quencher added. (b) Quenching efficiency was calculated by dividing the MFI signal of quenched over unquenched sample and expressing as a percentage. Experiments with each group were performed in duplicates and triplicates respectively (n = 2-3) ± standard deviation (SD).*

Next, we tested the sensor's ability to quench signal when added to HEK293 cells. The calculated quenching efficiency of QSY-Tet with HEK293 cells was observed to be slightly lower than with compensation beads, at ~60%. This could be due to VSVG protein mediated membrane fusion between the virus envelope and the host cellular membrane (110), hindering the quencher's ability to success bind to the fluorescent component on the cell surface. However, there were no significant statistical difference between the two values observed (two-tailed P-value = 0.11, unpaired *t* test). The consistency between the two groups suggest that the sensor functions as intended and can be used to accurately quantify viral internalisation. While the quenching efficiency for the sensor/quencher pair only needs to be determined once, it can be noted that including a 4^{o}C control in all experiments can improve the accuracy of the measurement by accounting for slight variations in the quenching efficiency. Since the key aspect of this project is to highlight the significance of HaloTag expression in the use of sensor conjugation on viruses, we found it adequate with just an initial calculation of the quenching efficiency as proof of optimal sensor activity.

Chapter Summary

HaloTag fusion proteins presents as a highly reactive, specific, and stable system for bio-orthogonal labelling in live cells and now lentiviruses. The impact of HaloTag incorporation and subsequent labelling with fluorescent internalisation sensor on both viral particle production and infectivity was determined. The former was assayed via nanoparticle tracking analysis (NTA), whereas the later was measured by quantifying gene delivery to cells via flow cytometry (transduction titre). Viral particle size was also observed to ensure minimal impact on the physiology of the labelled lentiviral vectors. All studies indicated that neither the production nor the gene delivery function of labelled lentiviral vectors was significantly affected by the genetically incorporated HaloTag fusion protein and internalisation sensor.

Subsequent observations of sensor function and activity in solution was performed before quantifying internalisation in cells. The labelling intensity of the internalisation sensor was observed by incubating flow cytometry compensation beads at various ratios and various lengths of time with the labelled lentiviral vectors. This allowed us to determine the fluorescence intensity of a single virion particle and correlate the number of viral particles internalised within cells for future experiments. The quenching efficiency of the Tet quencher was also observed in solution using a fluorescence spectrophotometer before proceeding to in vitro quenching with both compensation beads and HEK293 cells (Appendix C). Quenching efficiency of the Tet quencher was comparable to data presented by Fitzgerald et al. (2018) (~85%) and while there were slight differences in efficiencies between compensation beads and HEK293 cells, there was no statistical significance observed.

In summary, internalisation sensor labelled lentiviral vectors functions as intended and can be used to accurately quantify internalisation of viruses in cells. In addition, the sensor is highly specific and can be quenched efficiently with the presence of the quencher component. The presence of the sensor on the lentiviral surface has minimal effects on viral production and infectivity as demonstrated by these studies and presents an opportunity to observe viral internalisation over time.

Chapter 5. Uptake and Internalisation Studies

Abstract

In previous chapters, synthesis of HaloTag expressed lentiviruses and validation of Halo-sCy5-TCO internalisation sensor activity and quenching efficiency were demonstrated using compensation beads and *in vitro* in HEK293 cells. In this chapter, the final aims of observing viral internalisation of the labelled lentiviruses in HEK293 cells *in vitro* across multiple time points were addressed. Here, we investigate viral association and binding, distinguishing these processes from internalisation and fusion of viruses during host cell entry with the use of the internalisation sensor. This chapter also includes data correlating fluorescence intensities from the fluorescent component of the internalisation sensor with the number of viruses internalised within individual cells. This method allows to dissect and to independently detect viral binding and internalisation during host cell entry, exploring the efficiencies and pitfalls of overall entry and replication processes of VSVG pseudotyped lentiviral vectors as well as potential rate limiting steps that hinders effective gene transduction once internalised.

5.1 Viral Uptake and Internalisation

Viruses are the most abundant intracellular pathogens and are entirely dependent on host cells to replicate their genomes. Understanding the viral life cycle and studying the cellular mechanisms in viral infection are crucial for the identification of new antiviral targets and allow the development of antiviral drugs. This knowledge also presents a useful area of interest for drug delivery systems due to their innate ability to avoid the immune system and enter cells. Currently, methods for studying viral entry vary greatly, and often rely solely on post-entry parameters, such as expression of a reporter gene, rather than on measuring entry *per se*. Research viral entry directly, i.e., in a virus replication-independent manner, has been challenging, even more so when using low, physiologically relevant amounts of viral particles.

In this chapter, assays to observe viral binding and internalisation using a fluorescent internalisation sensor using HaloTag fusion proteins has been observed in HEK293 cells, in which a quencher component was added to cells post incubation to remove extracellular signal.

5.1.1 Viral Internalisation Efficiency in HEK293 Cells

Briefly, a multiplicity of infection (MOI) of 5 of lentiviruses to HEK293 cells were incubated as a parameter for the prediction of fluorescent gene transfer. The various incubation time points were 5 minutes, 15 minutes, 30 minutes, 1 hour, 2 hours, 24 hours, and 48 hours respectively before being measured using flow cytometry. The internalisation efficiency equation and experimental flowchart is as described in Chapter 2, section 2.4.1 Quenching Efficiency and Internalisation and section 2.4.2 Experimental Design and Flowchart respectively.

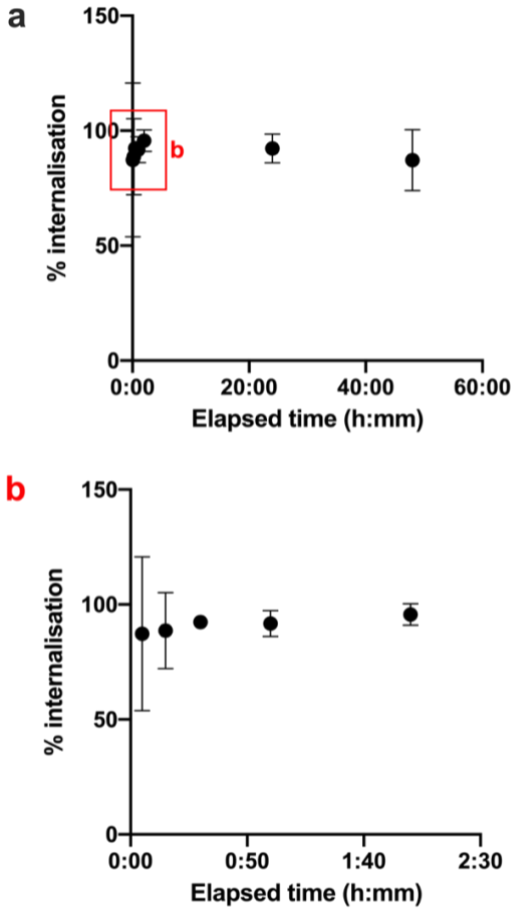

	5 min	15 min	30 min	1h	2h	24h	48h
%	87.3 ±	88.7 ±	92.3 ±	91.8 ±	95.6 ±	92.3 ±	87.2 ±
Internalised	34	17	3.0	5.7	4.6	6.3	13

Figure 5-1 ***Viral particles are rapidly internalised within minutes of incubation.*** *Quantifying percentage of internalised viruses in HEK293 cells up to 48 hours. Percentage internalisation is calculated based on Cy5 signal of internalisation sensor using the equation developed by Fitzgerald et al (2018) (80). (a) Percentage of internalised viruses after 5 minutes, 15 minutes, 30 minutes, 1 hour, 2 hour, 24 hours and 48 hours respectively. Inset graph (b) included to highlight percentage of internalised viruses after 5 minutes, 15 minutes, 30 minutes, 1 hour and 2 hour respectively. Each time points were performed in triplicates (n=3) ± standard deviation (SD).*

Majority of VSV glycoproteins undergo receptor mediated endocytosis through low-density lipoprotein receptors (LDL) (111) and can rapidly enter the cell, as seen in Figure 5-1 whereby only 5 minutes of incubation with HEK293 cells resulted in an average calculation of 87.3 ± 19.3% internalisation. While percentage internalised slowly increased over time, there was no statistical difference (P = 0.9915, one-way ANOVA) in the final amount of viral uptake at 48h. These results demonstrated that effective viral uptake and internalisation occurs with HEK293 cells and further supports other studies that observes a similar response with engineered lentiviral vectors (51, 66).

While the internalisation sensor has been used previously for observing nanoparticle and antibody internalisation, this initial insight into viral internalisation using a molecular sensor presents the use of an adaptor system with these tools as a versatile way to probe uptake and endocytosis. It should also be noted that despite the quenching efficiency of the molecular sensor is slightly lower than anticipated, the uptake kinetics observed, and subsequent sensitivity of the assay is unlikely to be affected due to the rapid uptake of the lentiviruses.

Viral entry is a highly dynamic process that includes multiple steps, including virus-receptor interactions, internalisation, endosomal escape, and finally nuclear transport. There are also viral transfection steps such as packaging and assembly of viral proteins that have consequential effects in establishing successful infections. This internalisation assay demonstrates efficient and rapid viral endocytosis with the use of molecular sensors, and the next step of this research should be focused on probing endosomal fusion and escape as potential limiting factors of successful gene transduction.

5.2 Correlating Number of Labelled Viral Particles with Transduction Efficiency

The number of viruses internalised from these assays can be correlated based on the labelling efficiency assay determined with compensation beads in Chapter 4.3.1 Optimising Sensor Activity Assay with Compensation Beads. Each individual labelled viruses can be detected with the fluorescence intensity measured from the internalisation sensor and is demonstrated in Figure 5-2, where HEK293 cells that are expressing mEmerald GFP would contain lentiviruses that have been successfully internalised.

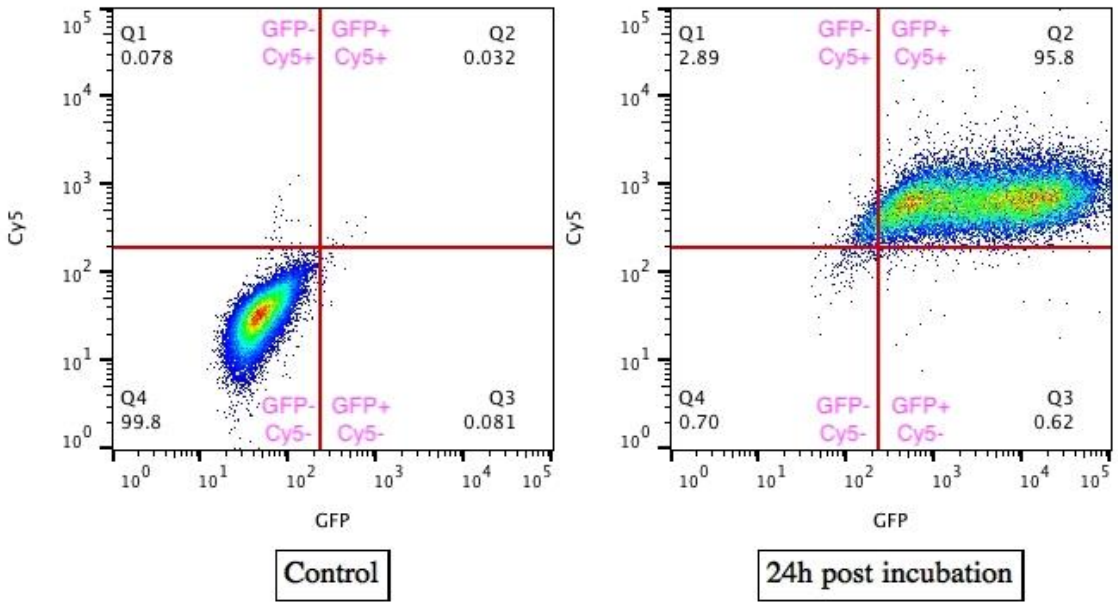

Figure 5-2 ***Sensor labelled lentiviruses observes successful internalisation, endosomal escape, and subsequent replication of transfer mEmerald GFP reporter gene.*** *Representative flow cytometric plots of HEK293 cells incubated with labelled lentiviruses showing GFP versus Cy5. The plot on the left and right represents the control and 24 h post incubation group respectively. Quadrants Q1 – Q4 represent cells with the phenotypes of $GFP^-/Cy5^+$, $GFP^+/Cy5^+$, $GFP^-/Cy5^-$, and $GFP^+/Cy5^-$, respectively. The percentage of cells conferring each phenotype is indicated in its respective quadrant.*

From Equation 4, each sample's respective Cy5 fluorescence intensity was correlated to number of viruses internalised and plotted across the multiple incubation times as seen in Figure 5-3. Baseline fluorescence was subtracted before applying the equation to account for noise and potential autofluorescence and a trend of increasing number of viruses internalised could be observed, starting with the sample group of 5 minutes with an average of 89 particles slowly increasing to 96 particles after 15 minutes of incubation and so forth. The maximum number of internalised viruses detected was after 48 hours of incubation with approximately 45188 particles compared to an

average of 165 viruses and 5158 viruses internalised after 2 hours and 24 hours respectively.

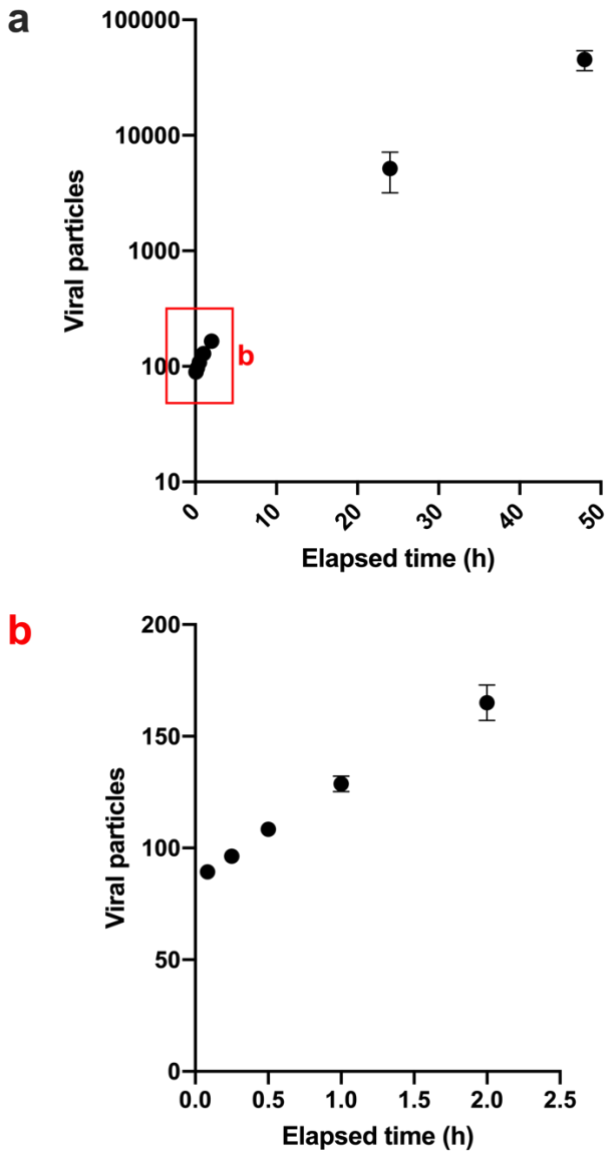

Figure 5-3 ***Viral particle uptake and internalisation increases signficantly over 48 hours.*** *Number of internalised viral particles calculated based on average Cy5 signal of labelled compensation beads. (a) Number of internalised viruses after 5 minutes, 15 minutes, 30 minutes, 1 hour, 2 hour, 24 hours and 48 hours respectively. Inset graph (b) included to highlight number of internalised viruses after 5 minutes, 15 minutes, 30 minutes, 1 hour and 2 hour respectively. Each time points were performed in triplicates (n=3) ± standard deviation (SD).*

Roughly 500,000 viruses were added to 100,000 HEK293 cells per well for a multiplicity of infection of 5 based on total physical concentration from nanoparticle tracking analysis. An estimated of only 9% of the total number of viruses that were internalised and able to efficiently transduce mEmerald GFP in cells despite initial internalisation of approximately 90%, further implicating the importance of viral escape, and trafficking in cells required for successful infection.

Different viruses are able to utilise different pathways for viral internalisation, in this instance the vesicular stomatitis virus (VSV) pseudotyped lentivirus relying on receptor mediated endocytosis with low-density lipoprotein receptor (LDL-R) family as the main pathway (112, 113).

The efficiency of viral internalisation demonstrated through this assay suggests that majority of the viral entry pathways are highly conducive and relevant, where even the same viruses might be able to enter diverse cells by several different routes (114). However, viral infectivity encompasses more than just the early entry steps, but also the critical processes involving gene transduction and replication.

Once internalised, viral particles would need to escape the endosomes and be localised and transported to the nucleus. Other than playing a distinct role in viral entry, the VSV membrane also mediates fusion between viral and endosomal membranes (115). Fusion is triggered by endosomal acidification, undergoing “viral uncoating” within early endosomes (116). While the internalisation sensor may not be able to disseminate the endosomal escape efficiency of viruses, the delayed expression of the mEmerald reporter gene suggests that membrane fusion and escape may potentially be another rate limiting step in addition to critical viral binding and uptake.

The combination of viral packaging, internalisation, endosomal escape, and localisation sums up the overall infectivity of the virus, with the internalisation sensor proving to be a useful tool in elucidating one of the many critical steps for successful replication. Overall, the versatility of the HaloTag fusion system is notably highlighted in this research, with the use of molecular sensors to further uncover viral internalisation without compromising viral function.

Briefly, one of the caveats of this assay is that that due to the expression of the HaloTag on the viral surface, this tracks the viral coating rather than the content and limits the assays to any endosomal escape processes. Another caveat also includes the slightly lower quenching efficiency of the molecular sensor. However, this can easily be overcome with the use of a different molecular sensor with better quenching efficiency. Overall, this assay proves to be a success in establishing a protocol for developing HaloTag expressed lentiviruses that can conjugate proteins, antibodies and/or sensors with the respective HaloTag linker is a precise and controlled manner

without affecting viral health and can uncover a number of fundamental questions regarding viral infection.

5.3 Future Impacts and Direction

Given the global impact of influenza on human health and the particular importance of the entry process for viral tropism, large efforts are being undertaken to further our understanding of viral entry into host cells. Molecular sensors have been demonstrated to be a powerful tool in uncovering efficiency of viral internalisation in consideration of fragile viral cargo. This assay may serve as a multi-faceted high throughput approach in labelling other molecular sensors that can elucidate different mechanisms, such as nuclear localisation and so forth, and can also be modified for other types of delivery systems, enabling us to generate the next generation of nanoparticles with improved therapeutic efficiency as well as providing a baseline standard for quantifying internalisation across different studies.

Potential future work could begin with including a more comprehensive characterisation and comparison of the assembled viruses, such as including a reverse transcription polymerase chain reaction (RT-PCR) detection assay to distinguish infectious viral particles from non-infectious RNA, that are present in virtually all viral assembly. This study would be able to fill the gap in determining and isolating the inefficiencies caused by the viral packaging processes rather than the internalisation or localisation steps. The strength of this combination is that it allows a more global view among alternative but different techniques and correlate the various factors and conditions that can affect viral viability.

Chapter Summary

The use of molecular sensors as well as the HaloTag adaptor system captures the dynamic process of viral binding and internalisation. Through the internalisation assay, internalisation efficiencies of labelled lentiviruses across multiple incubation times were determined and demonstrated rapid internalisation as supported in literature.

The number of internalised lentiviruses were also calculated using the fluorescence intensity of the internalisation sensor and the number of viruses internalised slowly increased over the course of 48 hours. In summary, the limitations of the assay included the slightly lower quenching efficiency of the molecular sensor that could affect the sensitivity of this assay, as well as the conjugation of the sensor on the viral coating rather than the viral load, which hinders the sensor to further observe and distinguish endosomal escape and localisation.

Viral infectivity is a dynamic multi-step process that begins with viral assembly and packaging, followed by association and internalisation, and finally viral escape and replication. Each processes faces their own set of challenges and elucidating each step of viral infectivity would increase the likelihood in developing better drug delivery systems and expand our knowledge of viral pathogenesis mechanisms.

Appendix

Appendix A

VSVG protein quantification from Typhoon Imaging using densitometric analysis on ImageJ

	25% HaloTag-VSVG tag	50% HaloTag-VSVG tag	100% HaloTag-VSVG tag
Relative area under the curve (AUC)	2922	3625	5082

Appendix B

One-way ANOVA of MFI in GFP and Cy5 channels respectively with lentiviruses expressing different ratios of HaloTag-VSVG tag.

MFI in GFP channel

ANOVA results | Multiple comparisons

Ordinary one-way ANOVA
Multiple comparisons

Tukey's multiple comparisons test	Mean Diff.	95.00% CI of diff.	Significant?	Summary	Adjusted P Value			
Control (100% wild type VSVG) vs. 25% HaloTag VSV-G	-279.0	-808.9 to 250.9	No	ns	0.3893	A-B		
Control (100% wild type VSVG) vs. 50% HaloTag VSV-G	793.7	263.8 to 1324	Yes	**	0.0059	A-C		
Control (100% wild type VSVG) vs. 100% HaloTag VSV-G	2197	1667 to 2726	Yes	****	<0.0001	A-D		
25% HaloTag VSV-G vs. 50% HaloTag VSV-G	1073	542.8 to 1603	Yes	***	0.0009	B-C		
25% HaloTag VSV-G vs. 100% HaloTag VSV-G	2476	1946 to 3005	Yes	****	<0.0001	B-D		
50% HaloTag VSV-G vs. 100% HaloTag VSV-G	1403	873.1 to 1933	Yes	***	0.0001	C-D		
Test details	**Mean 1**	**Mean 2**	**Mean Diff.**	**SE of diff.**	**n1**	**n2**	**q**	**DF**
Control (100% wild type VSVG) vs. 25% HaloTag VSV-G	2259	2538	-279.0	165.5	3	3	2.385	8
Control (100% wild type VSVG) vs. 50% HaloTag VSV-G	2259	1465	793.7	165.5	3	3	6.784	8
Control (100% wild type VSVG) vs. 100% HaloTag VSV-G	2259	62.37	2197	165.5	3	3	18.77	8
25% HaloTag VSV-G vs. 50% HaloTag VSV-G	2538	1465	1073	165.5	3	3	9.168	8
25% HaloTag VSV-G vs. 100% HaloTag VSV-G	2538	62.37	2476	165.5	3	3	21.16	8
50% HaloTag VSV-G vs. 100% HaloTag VSV-G	1465	62.37	1403	165.5	3	3	11.99	8

MFI in Cy5 channel

ANOVA results | Multiple comparisons

Ordinary one-way ANOVA
Multiple comparisons

Tukey's multiple comparisons test	Mean Diff.	95.00% CI of diff.	Significant?	Summary	Adjusted P Value			
Control (100% wild type VSVG) vs. 25% HaloTag VSV-G	-378.1	-446.3 to -309.9	Yes	****	<0.0001	A-B		
Control (100% wild type VSVG) vs. 50% HaloTag VSV-G	-304.7	-372.9 to -236.5	Yes	****	<0.0001	A-C		
Control (100% wild type VSVG) vs. 100% HaloTag VSV-G	-269.7	-337.9 to -201.5	Yes	****	<0.0001	A-D		
25% HaloTag VSV-G vs. 50% HaloTag VSV-G	73.33	5.134 to 141.5	Yes	*	0.0357	B-C		
25% HaloTag VSV-G vs. 100% HaloTag VSV-G	108.3	40.13 to 176.5	Yes	**	0.0042	B-D		
50% HaloTag VSV-G vs. 100% HaloTag VSV-G	35.00	-33.20 to 103.2	No	ns	0.4091	C-D		
Test details	**Mean 1**	**Mean 2**	**Mean Diff.**	**SE of diff.**	**n1**	**n2**	**q**	**DF**
Control (100% wild type VSVG) vs. 25% HaloTag VSV-G	14.77	392.8	-378.1	21.30	3	3	25.11	8
Control (100% wild type VSVG) vs. 50% HaloTag VSV-G	14.77	319.5	-304.7	21.30	3	3	20.24	8
Control (100% wild type VSVG) vs. 100% HaloTag VSV-G	14.77	284.5	-269.7	21.30	3	3	17.91	8
25% HaloTag VSV-G vs. 50% HaloTag VSV-G	392.8	319.5	73.33	21.30	3	3	4.870	8
25% HaloTag VSV-G vs. 100% HaloTag VSV-G	392.8	284.5	108.3	21.30	3	3	7.194	8
50% HaloTag VSV-G vs. 100% HaloTag VSV-G	319.5	284.5	35.00	21.30	3	3	2.324	8

Appendix C

The quenching efficiency of the Tet quencher in solution using a fluorescence spectrophotometer against blank control.

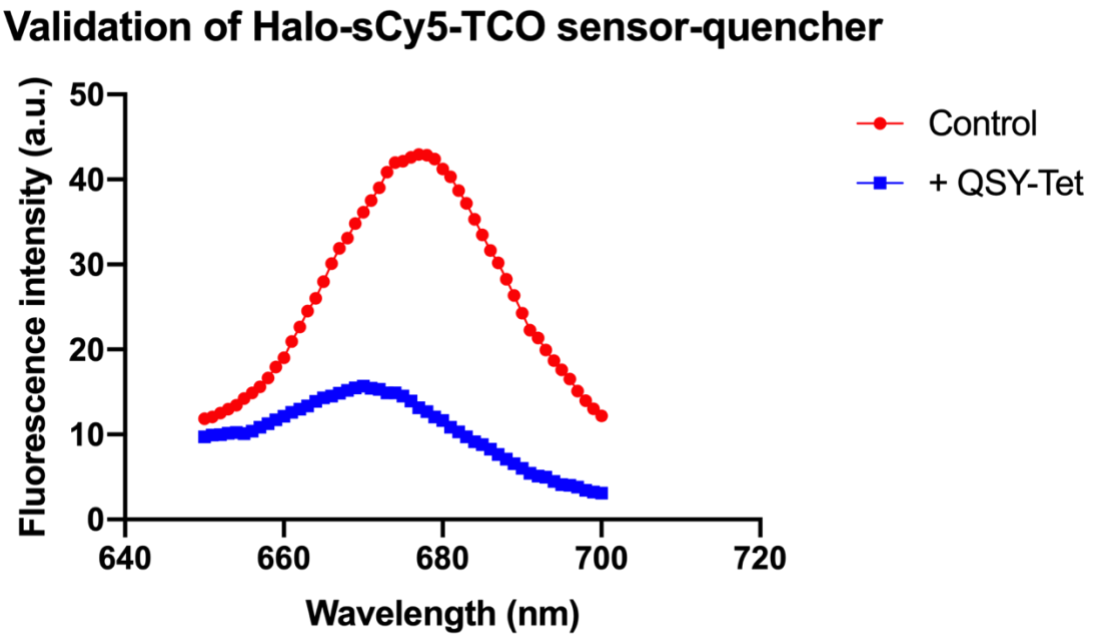

Appendix D

Gating strategy for analysing GFP positive or Cy5 positive HEK293 cells on FlowJo v.10

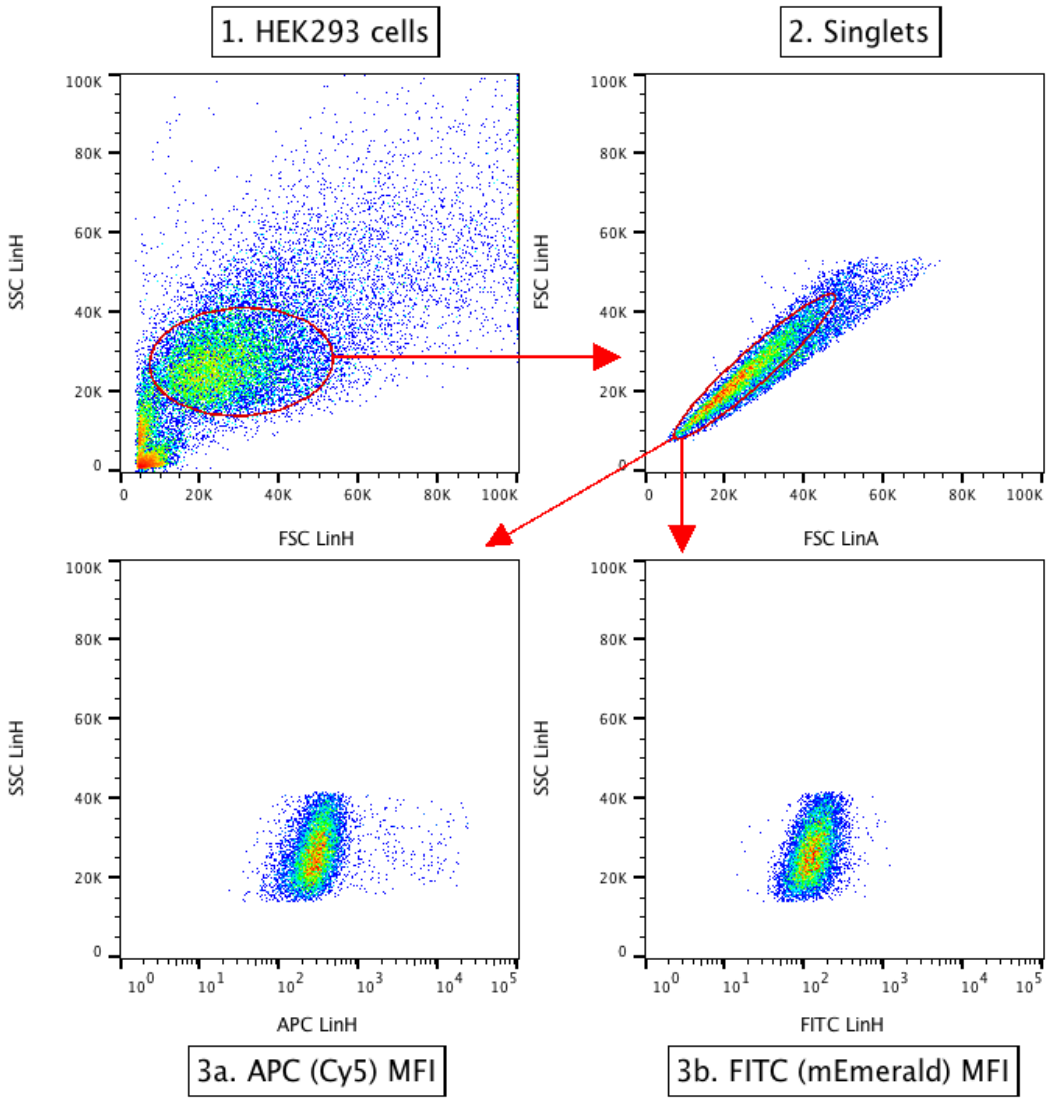

Appendix E

Representative summary reports from Nanoparticle Tracking Analysis (NTA) for total physical counts of lentiviruses

NANOSIGHT

25Halo 2020-07-31 10-43-16

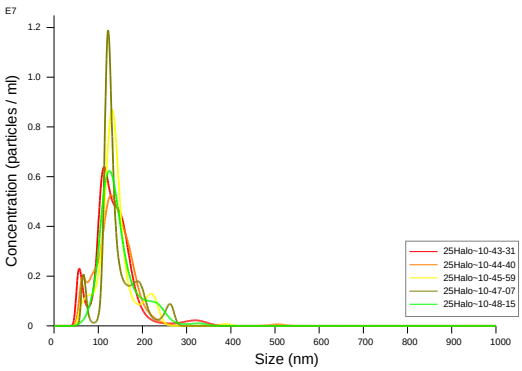

FTLA Concentration / Size graph for Experiment:
25Halo 2020-07-31 10-43-16

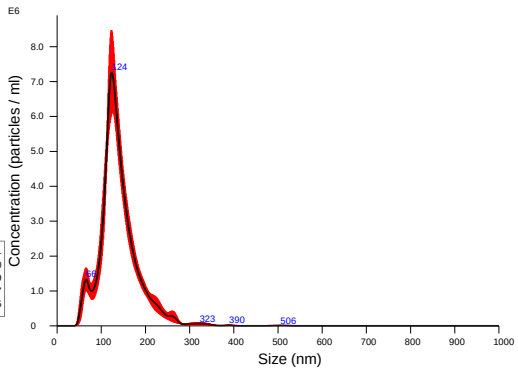

Averaged FTLA Concentration / Size for Experiment:
25Halo 2020-07-31 10-43-16
Error bars indicate + / -1 standard error of the mean

Included Files

25Halo 2020-07-31 10-43-31
25Halo 2020-07-31 10-44-40
25Halo 2020-07-31 10-45-59
25Halo 2020-07-31 10-47-07
25Halo 2020-07-31 10-48-15

Details

NTA Version:	NTA 3.4 Build 3.4.003
Script Used:	SOP Standard Measurement 10-43-16AM 31J~
Time Captured:	10:43:16 31/07/2020
Operator:	Jia
Pre-treatment:	
Sample Name:	100WT VSVG
Diluent:	1.30 and 1.2
Remarks:	

Capture Settings

Camera Type:	sCMOS
Laser Type:	Red
Camera Level:	12
Slider Shutter:	1200
Slider Gain:	146
FPS	25.0
Number of Frames:	1498
Temperature:	22.9 - 23.1 ^{o}C
Viscosity:	(Water) 0.928 - 0.934 cP
Dilution factor:	Dilution not recorded
Syringe Pump Speed:	40

Analysis Settings

Detect Threshold:	4
Blur Size:	Auto
Max Jump Distance:	Auto: 12.1 - 13.2 pix

Results

Stats: Merged Data

Mean:	139.7 nm
Mode:	123.6 nm
SD:	45.2 nm
D10:	93.3 nm
D50:	132.3 nm
D90:	194.7 nm

Stats: Mean +/- Standard Error

Mean:	139.8 +/- 2.0 nm
Mode:	124.2 +/- 3.2 nm
SD:	44.9 +/- 1.4 nm
D10:	94.3 +/- 5.5 nm
D50:	132.4 +/- 1.3 nm
D90:	195.7 +/- 5.8 nm
Concentration (Upgrade):	4.78e+08 +/- 8.97e+06 particles/ml
	27.9 +/- 0.4 particles/frame
	40.4 +/- 0.9 centres/frame

Concentration measurements may be unreliable
See summary file for more info

References

1. Lu W, Yao J, Zhu X, Qi Y. Nanomedicines: Redefining traditional medicine. Biomedicine & Pharmacotherapy. 2021;134:111103.
2. Lin J, Miao L, Zhong G, Lin C-H, Dargazangy R, Alexander-Katz A. Understanding the synergistic effect of physicochemical properties of nanoparticles and their cellular entry pathways. Communications Biology. 2020;3(1):205.
3. Blanco E, Shen H, Ferrari M. Principles of nanoparticle design for overcoming biological barriers to drug delivery. Nature Biotechnology. 2015;33(9):941-51.
4. Palanikumar L, Al-Hosani S, Kalmouni M, Nguyen VP, Ali L, Pasricha R, et al. pH-responsive high stability polymeric nanoparticles for targeted delivery of anticancer therapeutics. Communications Biology. 2020;3(1):95.
5. Deirram N, Zhang C, Kermaniyan SS, Johnston APR, Such GK. pH-Responsive Polymer Nanoparticles for Drug Delivery. Macromol Rapid Commun. 2019;40(10):e1800917.
6. Suk JS, Xu Q, Kim N, Hanes J, Ensign LM. PEGylation as a strategy for improving nanoparticle-based drug and gene delivery. Adv Drug Deliv Rev. 2016;99(Pt A):28-51.
7. Patsula V, Horák D, Kučka J, Macková H, Lobaz V, Francová P, et al. Synthesis and modification of uniform PEG-neridronate-modified magnetic nanoparticles determines prolonged blood circulation and biodistribution in a mouse preclinical model. Scientific Reports. 2019;9(1):10765.
8. Noyes AA, Whitney WR. The rate of solution of solid substances in their own solutions. Journal of the American Chemical Society. 1897;19(12):930-4.
9. Patra JK, Das G, Fraceto LF, Campos EVR, Rodriguez-Torres MdP, Acosta-Torres LS, et al. Nano based drug delivery systems: recent developments and future prospects. Journal of Nanobiotechnology. 2018;16(1):71.
10. Rees P, Wills JW, Brown MR, Barnes CM, Summers HD. The origin of heterogeneous nanoparticle uptake by cells. Nature Communications. 2019;10(1):2341.
11. Donahue ND, Acar H, Wilhelm S. Concepts of nanoparticle cellular uptake, intracellular trafficking, and kinetics in nanomedicine. Adv Drug Deliv Rev. 2019;143:68-96.
12. Wang W, Gaus K, Tilley RD, Gooding JJ. The impact of nanoparticle shape on cellular internalisation and transport: what do the different analysis methods tell us? Materials Horizons. 2019;6(8):1538-47.
13. Rennick JJ, Johnston APR, Parton RG. Key principles and methods for studying the endocytosis of biological and nanoparticle therapeutics. Nature Nanotechnology. 2021;16(3):266-76.
14. Behzadi S, Serpooshan V, Tao W, Hamaly MA, Alkawareek MY, Dreaden EC, et al. Cellular uptake of nanoparticles: journey inside the cell. Chem Soc Rev. 2017;46(14):4218-44.
15. Duncan R, Richardson SCW. Endocytosis and Intracellular Trafficking as Gateways for Nanomedicine Delivery: Opportunities and Challenges. Molecular Pharmaceutics. 2012;9(9):2380-402.
16. Gordon S. Phagocytosis: an immunobiologic process. Immunity. 2016;44(3):463-75.
17. Gustafson HH, Holt-Casper D, Grainger DW, Ghandehari H. Nanoparticle Uptake: The Phagocyte Problem. Nano Today. 2015;10(4):487-510.
18. Hillaireau H, Couvreur P. Nanocarriers' entry into the cell: relevance to drug delivery. Cell Mol Life Sci. 2009;66(17):2873-96.
19. Li Y-X, Pang H-B. Macropinocytosis as a cell entry route for peptide-functionalized and bystander nanoparticles. Journal of Controlled Release. 2021;329:1222-30.

20. Thottacherry JJ, Sathe M, Prabhakara C, Mayor S. Spoiled for Choice: Diverse Endocytic Pathways Function at the Cell Surface. Annual Review of Cell and Developmental Biology. 2019;35(1):55-84.
21. Bitsikas V, Corrêa Jr IR, Nichols BJ. Clathrin-independent pathways do not contribute significantly to endocytic flux. Elife. 2014;3:e03970.
22. Ehrlich M, Boll W, Van Oijen A, Hariharan R, Chandran K, Nibert ML, et al. Endocytosis by random initiation and stabilization of clathrin-coated pits. Cell. 2004;118(5):591-605.
23. Boucrot E, Ferreira AP, Almeida-Souza L, Debard S, Vallis Y, Howard G, et al. Endophilin marks and controls a clathrin-independent endocytic pathway. Nature. 2015;517(7535):460-5.
24. Howes MT, Kirkham M, Riches J, Cortese K, Walser PJ, Simpson F, et al. Clathrin-independent carriers form a high capacity endocytic sorting system at the leading edge of migrating cells. Journal of Cell Biology. 2010;190(4):675-91.
25. Hemalatha A, Prabhakara C, Mayor S. Endocytosis of Wingless via a dynamin-independent pathway is necessary for signaling in Drosophila wing discs. Proceedings of the National Academy of Sciences. 2016;113(45):E6993-E7002.
26. Sathe M, Muthukrishnan G, Rae J, Disanza A, Thattai M, Scita G, et al. Small GTPases and BAR domain proteins regulate branched actin polymerisation for clathrin and dynamin-independent endocytosis. Nature communications. 2018;9(1):1-16.
27. Parton RG, Collins BM. Unraveling the architecture of caveolae. Proceedings of the National Academy of Sciences. 2016;113(50):14170-2.
28. Parton RG. Caveolae: structure, function, and relationship to disease. Annual review of cell and developmental biology. 2018;34:111-36.
29. Parton RG, Del Pozo MA, Vassilopoulos S, Nabi IR, Le Lay S, Lundmark R, et al. Caveolae: The FAQs. Traffic. 2020;21(1):181-5.
30. Varkouhi AK, Scholte M, Storm G, Haisma HJ. Endosomal escape pathways for delivery of biologicals. Journal of Controlled Release. 2011;151(3):220-8.
31. Somiya M, Liu Q, Kuroda Si. Current Progress of Virus-mimicking Nanocarriers for Drug Delivery. Nanotheranostics. 2017;1(4):415-29.
32. Kotterman MA, Chalberg TW, Schaffer DV. Viral vectors for gene therapy: translational and clinical outlook. Annual review of biomedical engineering. 2015;17:63-89.
33. Parodi A, Molinaro R, Sushnitha M, Evangelopoulos M, Martinez JO, Arrighetti N, et al. Bio-inspired engineering of cell- and virus-like nanoparticles for drug delivery. Biomaterials. 2017;147:155-68.
34. Yoo J-W, Irvine DJ, Discher DE, Mitragotri S. Bio-inspired, bioengineered and biomimetic drug delivery carriers. Nature reviews Drug discovery. 2011;10(7):521-35.
35. Mercer J, Helenius A. Virus entry by macropinocytosis. Nature Cell Biology. 2009;11(5):510-20.
36. Yoo J, Park C, Yi G, Lee D, Koo H. Active Targeting Strategies Using Biological Ligands for Nanoparticle Drug Delivery Systems. Cancers (Basel). 2019;11(5).
37. Burns JC, Friedmann T, Driever W, Burrascano M, Yee J-K. Vesicular stomatitis virus G glycoprotein pseudotyped retroviral vectors: concentration to very high titer and efficient gene transfer into mammalian and nonmammalian cells. Proceedings of the National Academy of Sciences. 1993;90(17):8033-7.
38. Lay Mendoza MF, Acciani MD, Levit CN, Santa Maria C, Brindley MA. Monitoring Viral Entry in Real-Time Using a Luciferase Recombinant Vesicular Stomatitis Virus Producing SARS-CoV-2, EBOV, LASV, CHIKV, and VSV Glycoproteins. Viruses. 2020;12(12).

39. Burkard C, Bloyet L-M, Wicht O, van Kuppeveld FJ, Rottier PJM, de Haan CAM, et al. Dissecting virus entry: replication-independent analysis of virus binding, internalization, and penetration using minimal complementation of β-galactosidase. PLoS One. 2014;9(7):e101762-e.
40. Liu S-L, Wang Z-G, Xie H-Y, Liu A-A, Lamb DC, Pang D-W. Single-Virus Tracking: From Imaging Methodologies to Virological Applications. Chemical Reviews. 2020;120(3):1936-79.
41. Xu H, Hao X, Wang S, Wang Z, Cai M, Jiang J, et al. Real-time imaging of rabies virus entry into living vero cells. Scientific reports. 2015;5(1):1-12.
42. Costantini LM, Snapp EL. Going Viral with Fluorescent Proteins. J Virol. 2015;89(19):9706-8.
43. FitzGerald LI, Johnston APR. It's what's on the inside that counts: Techniques for investigating the uptake and recycling of nanoparticles and proteins in cells. Journal of Colloid and Interface Science. 2021;587:64-78.
44. Vangindertael J, Camacho R, Sempels W, Mizuno H, Dedecker P, Janssen K. An introduction to optical super-resolution microscopy for the adventurous biologist. Methods and applications in fluorescence. 2018;6(2):022003.
45. Dunn KW, Kamocka MM, McDonald JH. A practical guide to evaluating colocalization in biological microscopy. American Journal of Physiology-Cell Physiology. 2011;300(4):C723-C42.
46. Huang F-K, Chen W-C, Lai S-F, Liu C-J, Wang C-L, Wang C-H, et al. Enhancement of irradiation effects on cancer cells by cross-linked dextran-coated iron oxide (CLIO) nanoparticles. Physics in Medicine & Biology. 2009;55(2):469.
47. Rieseberg M, Kasper C, Reardon KF, Scheper T. Flow cytometry in biotechnology. Applied microbiology and biotechnology. 2001;56(3):350-60.
48. Sawyer ST, Krantz SB. Transferrin receptor number, synthesis, and endocytosis during erythropoietin-induced maturation of Friend virus-infected erythroid cells. Journal of Biological Chemistry. 1986;261(20):9187-95.
49. Austin CD, De Mazière AM, Pisacane PI, van Dijk SM, Eigenbrot C, Sliwkowski MX, et al. Endocytosis and sorting of ErbB2 and the site of action of cancer therapeutics trastuzumab and geldanamycin. Molecular biology of the cell. 2004;15(12):5268-82.
50. Naqvi SAR, Sosabowski JK, Nagra SA, Ishfaq MM, Mather SJ, Matzow T. Radiopeptide internalisation and externalisation assays: cell viability and radioligand integrity. Applied Radiation and Isotopes. 2011;69(1):68-74.
51. Ojima M, Tsuji K, Otabe K, Horie M, Koga H, Sekiya I, et al. Different methods of detaching adherent cells significantly affect the detection of stem cell antigens in synovial mesenchymal stem cells. Osteoarthritis and Cartilage. 2016;24:S509-S10.
52. Zhang B, Shan H, Li D, Li Z-r, Zhu K-s, Jiang Z-b, et al. Different methods of detaching adherent cells significantly affect the detection of TRAIL receptors. Tumori Journal. 2012;98(6):800-3.
53. Finnemann SC, Bonilha VL, Marmorstein AD, Rodriguez-Boulan E. Phagocytosis of rod outer segments by retinal pigment epithelial cells requires αvβ5 integrin for binding but not for internalization. Proceedings of the National Academy of Sciences. 1997;94(24):12932-7.
54. Nuutila J, Lilius EM. Flow cytometric quantitative determination of ingestion by phagocytes needs the distinguishing of overlapping populations of binding and ingesting cells. Cytometry Part A. 2005;65(2):93-102.
55. Strober W. Trypan Blue Exclusion Test of Cell Viability. Curr Protoc Immunol. 2015;111:A3.B.1-A3.B.

56. Tan YF, Mundargi RC, Chen MHA, Lessig J, Neu B, Venkatraman SS, et al. Layer-by-layer nanoparticles as an efficient siRNA delivery vehicle for SPARC silencing. Small. 2014;10(9):1790-8.
57. Kakimoto S, Hamada T, Komatsu Y, Takagi M, Tanabe T, Azuma H, et al. The conjugation of diphtheria toxin T domain to poly (ethylenimine) based vectors for enhanced endosomal escape during gene transfection. Biomaterials. 2009;30(3):402-8.
58. Van Amersfoort ES, Van Strijp JA. Evaluation of a flow cytometric fluorescence quenching assay of phagocytosis of sensitized sheep erythrocytes by polymorphonuclear leukocytes. Cytometry: The Journal of the International Society for Analytical Cytology. 1994;17(4):294-301.
59. Nath N, Godat B, Zimprich C, Dwight SJ, Corona C, McDougall M, et al. Homogeneous plate based antibody internalization assay using pH sensor fluorescent dye. J Immunol Methods. 2016;431:11-21.
60. Göstring L, Chew MT, Orlova A, Höidén-Guthenberg I, Wennborg A, Carlsson J, et al. Quantification of internalization of EGFR-binding Affibody molecules: Methodological aspects. International journal of oncology. 2010;36(4):757-63.
61. Whitaker JE, Haugland RP, Prendergast FG. Spectral and photophysical studies of benzo [c] xanthene dyes: dual emission pH sensors. Analytical biochemistry. 1991;194(2):330-44.
62. Vira S, Mekhedov E, Humphrey G, Blank PS. Fluorescent-labeled antibodies: Balancing functionality and degree of labeling. Analytical biochemistry. 2010;402(2):146-50.
63. Liu H, Johnston AP. A programmable sensor to probe the internalization of proteins and nanoparticles in live cells. Angewandte Chemie. 2013;125(22):5856-60.
64. Dautry-Varsat A, Ciechanover A, Lodish HF. pH and the recycling of transferrin during receptor-mediated endocytosis. Proceedings of the National Academy of Sciences. 1983;80(8):2258-62.
65. Mayle KM, Le AM, Kamei DT. The intracellular trafficking pathway of transferrin. Biochimica et Biophysica Acta (BBA)-General Subjects. 2012;1820(3):264-81.
66. Chu Y, Oum YH, Carrico IS. Surface modification via strain-promoted click reaction facilitates targeted lentiviral transduction. Virology. 2016;487:95-103.
67. Metzner C, Kochan F, Dangerfield JA. Postexit Surface Engineering of Retroviral/Lentiviral Vectors. BioMed Research International. 2013;2013:253521.
68. Lee DY, Cha B-H, Jung M, Kim AS, Bull DA, Won Y-W. Cell surface engineering and application in cell delivery to heart diseases. Journal of Biological Engineering. 2018;12(1):28.
69. Suleiman E, Mayer J, Lehner E, Kohlhauser B, Katholnig A, Batzoni M, et al. Conjugation of Native-Like HIV-1 Envelope Trimers onto Liposomes Using EDC/Sulfo-NHS Chemistry: Requirements and Limitations. Pharmaceutics. 2020;12(10).
70. Gabal Y, Ramsey JD. Surface Modification of Adenovirus Vector to Improve Immunogenicity and Tropism. In: Pfeifer BA, Hill A, editors. Vaccine Delivery Technology: Methods and Protocols. New York, NY: Springer US; 2021. p. 357-66.
71. Ratnatilaka Na Bhuket P, Luckanagul JA, Rojsitthisak P, Wang Q. Chemical modification of enveloped viruses for biomedical applications. Integr Biol (Camb). 2018;10(11):666-79.
72. Müller TG, Sakin V, Müller B. A Spotlight on Viruses-Application of Click Chemistry to Visualize Virus-Cell Interactions. Molecules. 2019;24(3):481.
73. Duvergé A, Negroni M. Pseudotyping Lentiviral Vectors: When the Clothes Make the Virus. Viruses. 2020;12(11).

74. Henry S, Williams E, Barr K, Korchagina E, Tuzikov A, Ilyushina N, et al. Rapid one-step biotinylation of biological and non-biological surfaces. Scientific Reports. 2018;8(1):2845.
75. Hadac EM, Federspiel MJ, Chernyy E, Tuzikov A, Korchagina E, Bovin NV, et al. Fluorescein and radiolabeled Function-Spacer-Lipid constructs allow for simple in vitro and in vivo bioimaging of enveloped virions. J Virol Methods. 2011;176(1-2):78-84.
76. Ratnatilaka Na Bhuket P, Luckanagul JA, Rojsitthisak P, Wang Q. Chemical modification of enveloped viruses for biomedical applications. Integrative Biology. 2018;10(11):666-79.
77. Schmid M, Ernst P, Honegger A, Suomalainen M, Zimmermann M, Braun L, et al. Adenoviral vector with shield and adapter increases tumor specificity and escapes liver and immune control. Nature Communications. 2018;9(1):450.
78. Capasso C, Hirvinen M, Cerullo V. Beyond Gene Delivery: Strategies to Engineer the Surfaces of Viral Vectors. Biomedicines. 2013;1(1):3-16.
79. Waehler R, Russell SJ, Curiel DT. Engineering targeted viral vectors for gene therapy. Nature Reviews Genetics. 2007;8(8):573-87.
80. Selby LI, Aurelio L, Yuen D, Graham B, Johnston APR. Quantifying Cellular Internalization with a Fluorescent Click Sensor. ACS Sensors. 2018;3(6):1182-9.
81. Lippé R. Flow Virometry: a Powerful Tool To Functionally Characterize Viruses. J Virol. 2018;92(3).
82. Lim CY, Owens NA, Wampler RD, Ying Y, Granger JH, Porter MD, et al. Succinimidyl Ester Surface Chemistry: Implications of the Competition between Aminolysis and Hydrolysis on Covalent Protein Immobilization. Langmuir. 2014;30(43):12868-78.
83. Lim CY, Owens NA, Wampler RD, Ying Y, Granger JH, Porter MD, et al. Succinimidyl ester surface chemistry: implications of the competition between aminolysis and hydrolysis on covalent protein immobilization. Langmuir : the ACS journal of surfaces and colloids. 2014;30(43):12868-78.
84. Cronin J, Zhang X-Y, Reiser J. Altering the tropism of lentiviral vectors through pseudotyping. Current gene therapy. 2005;5(4):387-98.
85. Chojnacki J, Waithe D, Carravilla P, Huarte N, Galiani S, Enderlein J, et al. Envelope glycoprotein mobility on HIV-1 particles depends on the virus maturation state. Nature communications. 2017;8(1):545-.
86. Croyle MA, Callahan SM, Auricchio A, Schumer G, Linse KD, Wilson JM, et al. PEGylation of a vesicular stomatitis virus G pseudotyped lentivirus vector prevents inactivation in serum. J Virol. 2004;78(2):912-21.
87. Wen AM, Infusino M, De Luca A, Kernan DL, Czapar AE, Strangi G, et al. Interface of physics and biology: engineering virus-based nanoparticles for biophotonics. Bioconjug Chem. 2015;26(1):51-62.
88. Dempsey DR, Jiang H, Kalin JH, Chen Z, Cole PA. Site-Specific Protein Labeling with N-Hydroxysuccinimide-Esters and the Analysis of Ubiquitin Ligase Mechanisms. Journal of the American Chemical Society. 2018;140(30):9374-8.
89. Liu S, Kondo N, Long Y, Xiao D, Iwamoto A, Matsuda Z. Membrane topology analysis of HIV-1 envelope glycoprotein gp41. Retrovirology. 2010;7(1):100.
90. Wang H, Li X, Nakane S, Liu S, Ishikawa H, Iwamoto A, et al. Co-expression of foreign proteins tethered to HIV-1 envelope glycoprotein on the cell surface by introducing an intervening second membrane-spanning domain. PLoS One. 2014;9(5):e96790-e.
91. Sun X, Zhang A, Baker B, Sun L, Howard A, Buswell J, et al. Development of SNAP-Tag Fluorogenic Probes for Wash-Free Fluorescence Imaging. ChemBioChem. 2011;12(14):2217-26.

92. Los GV, Encell LP, McDougall MG, Hartzell DD, Karassina N, Zimprich C, et al. HaloTag: a novel protein labeling technology for cell imaging and protein analysis. ACS Chem Biol. 2008;3(6):373-82.
93. Los GV, Encell LP, McDougall MG, Hartzell DD, Karassina N, Zimprich C, et al. HaloTag: A Novel Protein Labeling Technology for Cell Imaging and Protein Analysis. ACS Chemical Biology. 2008;3(6):373-82.
94. Prato M, Marchesan S. ChemInform Abstract: Under the Lens: Carbon Nanotube and Protein Interaction at the Nanoscale. Chem Commun. 2015;51.
95. Hastie E, Cataldi M, Marriott I, Grdzelishvili VZ. Understanding and altering cell tropism of vesicular stomatitis virus. Virus Res. 2013;176(1-2):16-32.
96. Merten O-W, Hebben M, Bovolenta C. Production of lentiviral vectors. Mol Ther Methods Clin Dev. 2016;3:16017-.
97. Farley DC, Iqball S, Smith JC, Miskin JE, Kingsman SM, Mitrophanous KA. Factors that influence VSV-G pseudotyping and transduction efficiency of lentiviral vectors—in vitro and in vivo implications. The Journal of Gene Medicine: A cross-disciplinary journal for research on the science of gene transfer and its clinical applications. 2007;9(5):345-56.
98. Wang X, McManus M. Lentivirus production. Journal of visualized experiments: JoVE. 2009(32).
99. Milone MC, O'Doherty U. Clinical use of lentiviral vectors. Leukemia. 2018;32(7):1529-41.
100. Frecha C, Szécsi J, Cosset FL, Verhoeyen E. Strategies for targeting lentiviral vectors. Curr Gene Ther. 2008;8(6):449-60.
101. Ilagan RP, Rhoades E, Gruber DF, Kao H-T, Pieribone VA, Regan L. A new bright green-emitting fluorescent protein--engineered monomeric and dimeric forms. FEBS J. 2010;277(8):1967-78.
102. Storck A, Ludtke J, Kopp L, Juckem L. Development and Optimization of a High Titer Recombinant Lentivirus System. BioTechniques. 2017;63(3):136-8.
103. Joo K-I, Fang Y, Liu Y, Xiao L, Gu Z, Tai A, et al. Enhanced real-time monitoring of adeno-associated virus trafficking by virus-quantum dot conjugates. ACS nano. 2011;5(5):3523-35.
104. Perry C, Rayat ACME. Lentiviral Vector Bioprocessing. Viruses. 2021;13(2):268.
105. Delenda C, Gaillard C. Real-time quantitative PCR for the design of lentiviral vector analytical assays. Gene Therapy. 2005;12(1):S36-S50.
106. Maguire CM, Rösslein M, Wick P, Prina-Mello A. Characterisation of particles in solution – a perspective on light scattering and comparative technologies. Science and Technology of Advanced Materials. 2018;19(1):732-45.
107. Marozsan AJ, Fraundorf E, Abraha A, Baird H, Moore D, Troyer R, et al. Relationships between infectious titer, capsid protein levels, and reverse transcriptase activities of diverse human immunodeficiency virus type 1 isolates. J Virol. 2004;78(20):11130-41.
108. Plantin J, Massanella M, Chomont N. Inducible HIV RNA transcription assays to measure HIV persistence: pros and cons of a compromise. Retrovirology. 2018;15(1):9.
109. Dimitrov D, Willey R, Sato H, Chang L-J, Blumenthal R, Martin M. Quantitation of human immunodeficiency virus type 1 infection kinetics. J Virol. 1993;67(4):2182-90.
110. Ci Y, Yang Y, Xu C, Shi L. Vesicular stomatitis virus G protein transmembrane region is crucial for the hemi-fusion to full fusion transition. Scientific Reports. 2018;8(1):10669.

111. Nikolic J, Belot L, Raux H, Legrand P, Gaudin Y, A Albertini A. Structural basis for the recognition of LDL-receptor family members by VSV glycoprotein. Nature communications. 2018;9(1):1029-.
112. Blaas D. Viral entry pathways: the example of common cold viruses. Wien Med Wochenschr. 2016;166(7-8):211-26.
113. Finkelshtein D, Werman A, Novick D, Barak S, Rubinstein M. LDL receptor and its family members serve as the cellular receptors for vesicular stomatitis virus. Proceedings of the National Academy of Sciences. 2013;110(18):7306-11.
114. Liu J, Yu C, Gui J-F, Pang D-W, Zhang Q-Y. Real-Time Dissecting the Entry and Intracellular Dynamics of Single Reovirus Particle. Frontiers in Microbiology. 2018;9(2797).
115. Beilstein F, Abou Hamdan A, Raux H, Belot L, Ouldali M, Albertini AA, et al. Identification of a pH-Sensitive Switch in VSV-G and a Crystal Structure of the G Pre-fusion State Highlight the VSV-G Structural Transition Pathway. Cell Rep. 2020;32(7):108042.
116. Li S, Sieben C, Ludwig K, Höfer CT, Chiantia S, Herrmann A, et al. pH-Controlled two-step uncoating of influenza virus. Biophys J. 2014;106(7):1447-56.